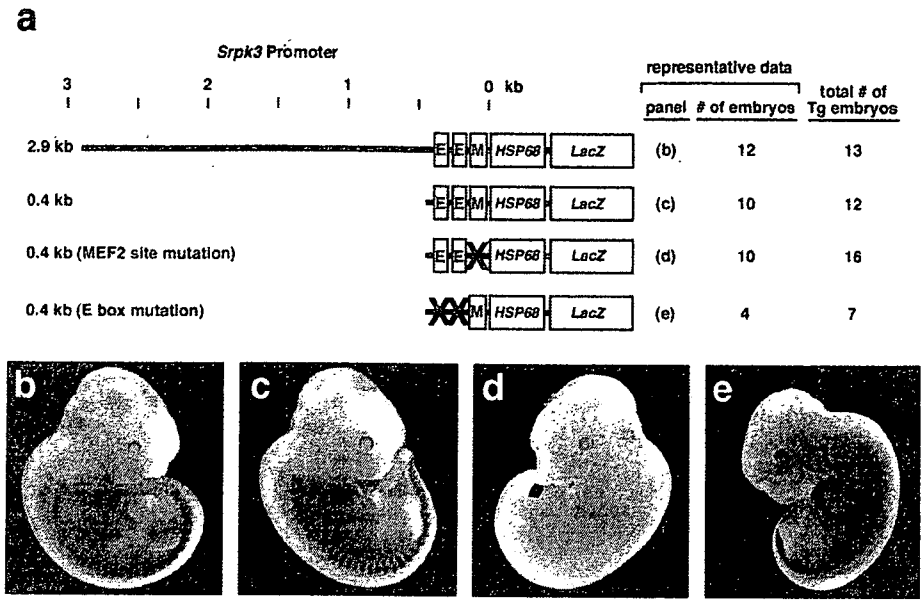

Figure 4. MEF2-dependent transcriptional control of Srpk3 in mouse embryos. (*a*) Schematic representation of *Srpk3-HSP68-LacZ* reporter constructs and results of F0 transgenic mouse analysis. The number of embryos that showed representative expression patterns and total transgenic embryos are shown on the *right*. Representative results are shown in panels *b–e*. The 2.9- and 0.4-kb fragments drove *LacZ* expression in the heart and somites in E11.5 embryos (*b,c,* respectively). The MEF2 site mutation (*d*), but not the E-box mutations (*e*), abolished the *LacZ* activity both in the heart and somites.

pressing Srpk3 in skeletal muscle, using the *muscle creatine kinase* (*MCK*) gene promoter and enhancer (Sternberg et al. 1988). Multiple F0 transgenic mice died prematurely with severe muscle wasting and growth retardation. Two F0 mice survived to sexual maturity and were fertile, but the F1 transgenic mice derived from these founders died at 2–8 wk of age, which prevented us from establishing transgenic mouse lines. However, those transgenic mice shared muscle defects with myofiber disarray and degeneration (Fig. 5a–c). These mice also showed myocyte regeneration characterized by an increase in centrally placed nuclei (Fig. 5c) and activation of embryonic gene markers (Fig. 5d). Although these characteristics are similar to those of muscular dystrophy, Evans Blue dye injection did not show abnormalities of sarcolemmal integrity (data not shown), and the expression of dystrophin and related sarcolemmal proteins was intact (Supplementary Fig. 2), suggesting that excess SRPK activity causes muscle degeneration by a different mechanism.

Centronuclear myopathy in Srpk3-null mice

To further elucidate the significance of Srpk3 in vivo, we generated *Srpk3*-null mice (Fig. 6a–c). The mutation we introduced into the gene deleted parts of exons 1 and 5 and all of exons 2, 3, and 4, which encode the N-terminal portion of Kinase Domain 1 (Fig. 6a). Northern analysis showed the complete absence of *Srpk3* transcripts in the heart and skeletal muscle of mutant mice (Fig. 6c).

Since the *Srpk3* gene is located on the X chromosome, wild-type and hemizygously null male mice were examined in this study. *Srpk3*-null mice were viable to adulthood, but displayed apparent defects in skeletal muscle growth. The mass of various skeletal muscle groups was significantly smaller than that of wild-type littermates at 1 mo (Fig. 6d) and 3 mo of age (data not shown). Histological analysis revealed a marked increase in centrally placed nuclei and a disorganized intermyofibrillar network, occasionally with ring-fiber-like structure or spheroid bodies (Fig. 6e,f; data not shown).

The pathological characteristics of *Srpk3*-null muscle were different from those of *MCK–Srpk3* transgenic mice. Although an increase in centrally placed nuclei is frequently indicative of muscle regeneration in response to disease or injury (Garry et al. 2000; Carpenter and Karpati 2001; Emery 2002), *Srpk3*-null mice did not show up-regulation of embryonic/perinatal muscle markers, which is typically seen during muscle regeneration (Fig. 6g). There were no signs of inflammation, neutrophil infiltration, or fibrosis in *Srpk3*-null mice (Fig. 6e), nor was there an increase in apoptotic cell death detectable by TUNEL staining (Fig. 6f). The serum creatine kinase activity indicative of sarcolemmal leakage also did not significantly increase in *Srpk3*-null mice (wild type, 409 ± 192; null, 486 ± 291; IU/L, $n = 10$), and Evans Blue dye injection did not show abnormalities of sarcolemmal integrity (Fig. 6f).

The pathological characteristics of the skeletal muscle in *Srpk3*-null mice, especially an increase of centronucleated myofibers without apparent myocyte death, are reminiscent of human centronuclear myopathy (Carpenter and Karpati 2001; Jeannet et al. 2004). However, centrally placed nuclei were observed only in type 2 fi-

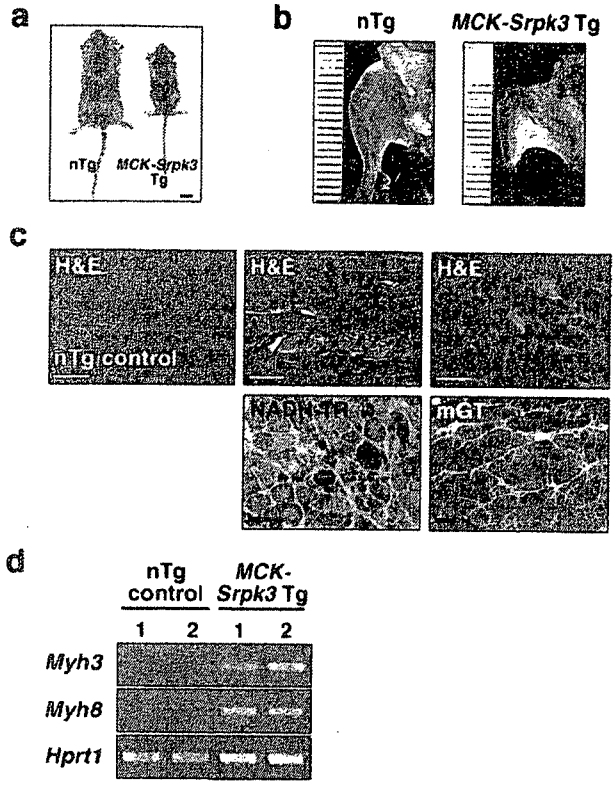

Figure 5. Muscle defects in *MCK–Srpk3* transgenic mice. (*a*,*b*) *Muscle creatine kinase* (*MCK*)–*Srpk3* transgenic (Tg) mice showed significant growth retardation and muscle defects compared with nontransgenic (nTg) littermates at 1 mo of age. Bar in panel *a* represents 1 cm. (*c*) Histological analysis of *MCK–Srpk3* Tg mice showed severe muscle degeneration with myofiber disarray, increase in centrally placed nuclei, and fibrosis. Hematoxylin & eosin (H&E), NADH-tetrazolium reductase (NADH-TR), and modified Gomori Trichrome (mGT) staining of gastrocnemius muscle. H&E staining of nTg control is also shown. Bar, 100 μm. (*d*) Muscle regeneration markers, *Myh3* and *Myh8*, are up-regulated in the skeletal muscle of *MCK–Srpk3* Tg mice. Similar results were obtained using F1 mice derived from two F0 founders of *MCK–Srpk3* transgenic mice.

bers, but not in type 1 fibers, in *Srpk3*-null mice (Fig. 6f), in contrast to type 1 fiber specific abnormalities associated with human centronuclear myopathy (Laporte et al. 1996; Carpenter and Karpati 2001; Jeannet et al. 2004). These results suggested that *Srpk3*-null mice displayed a new entity of centronuclear myopathy.

Alteration of muscle gene expression in Srpk3*-null mice*

To further characterize muscle abnormalities of *Srpk3*-null mice, we examined the expression of various muscle genes in type 2 fiber-enriched tibialis anterior muscles. A subset of type 1/slow fiber-enriched genes showed increased expression in *Srpk3*-null mice; however, the lack of activation of two representative slow-twitch fiber markers (Serrano et al. 2001; McCullagh et al. 2004), *Slc2a4/Glut4* and *Myoglobin* (*Mb*), suggests that the altered gene expression patterns are not a simple reflection of fiber type switching (Fig. 7a). Consistently, expression of type 2/fast fiber-enriched genes (Fig. 7a) as well as the proportions of type 1 and 2 fibers were not altered in *Srpk3*-null mice (wild type: type 1, 14.6%; type 2, 85.4%, $n = 700$; *Srpk3* null: type 1, 17.9%; type 2, 82.1%, $n = 800$).

Although there was a significant decrease of muscle mass in *Srpk3*-null mice, most atrophy-related genes (McKinnell and Rudnicki 2004) did not show alteration of expression in *Srpk3*-null mice. However, we observed a significant increase in expression of the *cartilage intermediate layer protein* (*Cilp*) gene (Fig. 7b), which encodes a secreted inhibitor of transforming growth factors and insulin-like growth factors (Lorenzo et al. 1998; Johnson et al. 2003; Seki et al. 2005). Given the importance of growth factor signaling in muscle diseases (McKinnell and Rudnicki 2004), up-regulation of *Cilp* expression may contribute, at least in part, to myopathy and muscle growth defects in *Srpk3*-null mice.

Calcium homeostasis plays critical roles in the regulation of skeletal muscle growth and contractility, and abnormalities in calcium handling have been implicated in various muscle diseases (MacLennan et al. 2003). Interestingly, mRNA expression of *Sarcolipin* (*Sln*) markedly increased in *Srpk3*-null mice (Fig. 7). Sln shares structural and functional similarity with Phospholamban, and they physically associate with and inhibit sarco(endo)plasmic reticulum calcium ATPase (Tupling et al. 2002; MacLennan et al. 2003). Forced expression of Sln in skeletal muscle represses sarcoplasmic reticulum calcium uptake and impairs contractile function (Tupling et al. 2002). Despite its important function, the expression patterns of *Sln* in muscle diseases have not been previously studied. We also observed that *Sln* expression increased in dystrophic Mdx mice as well as in cardiotoxin muscle injury models (Garry et al. 2000; Carpenter and Karpati 2001; Emery 2002; data not shown). How *Sln* expression is regulated in those conditions is unknown, but up-regulation of *Sln* expression may be a common characteristic of muscle diseases.

Discussion

MEF2 is a key regulator of cardiac and skeletal muscle development as well as remodeling of adult muscles in response to physiologic and pathologic signals (Black and Olson 1998; McKinsey et al. 2002). While MEF2 has been shown to regulate a wide range of muscle structural genes, few other target genes that might mediate its actions in muscle have been identified (Kuisk et al. 1996; Anderson et al. 2004; Phan et al. 2005). The results of the present study identify Srpk3 as a novel muscle-specific protein kinase, which is directly regulated by MEF2 and is essential for normal growth and homeostasis of skeletal muscle.

Abnormalities in skeletal muscle resulting from dysregulation of Srpk3

Striated muscles are highly sensitive to the level of Srpk3 expression. Overexpression of Srpk3 in skeletal

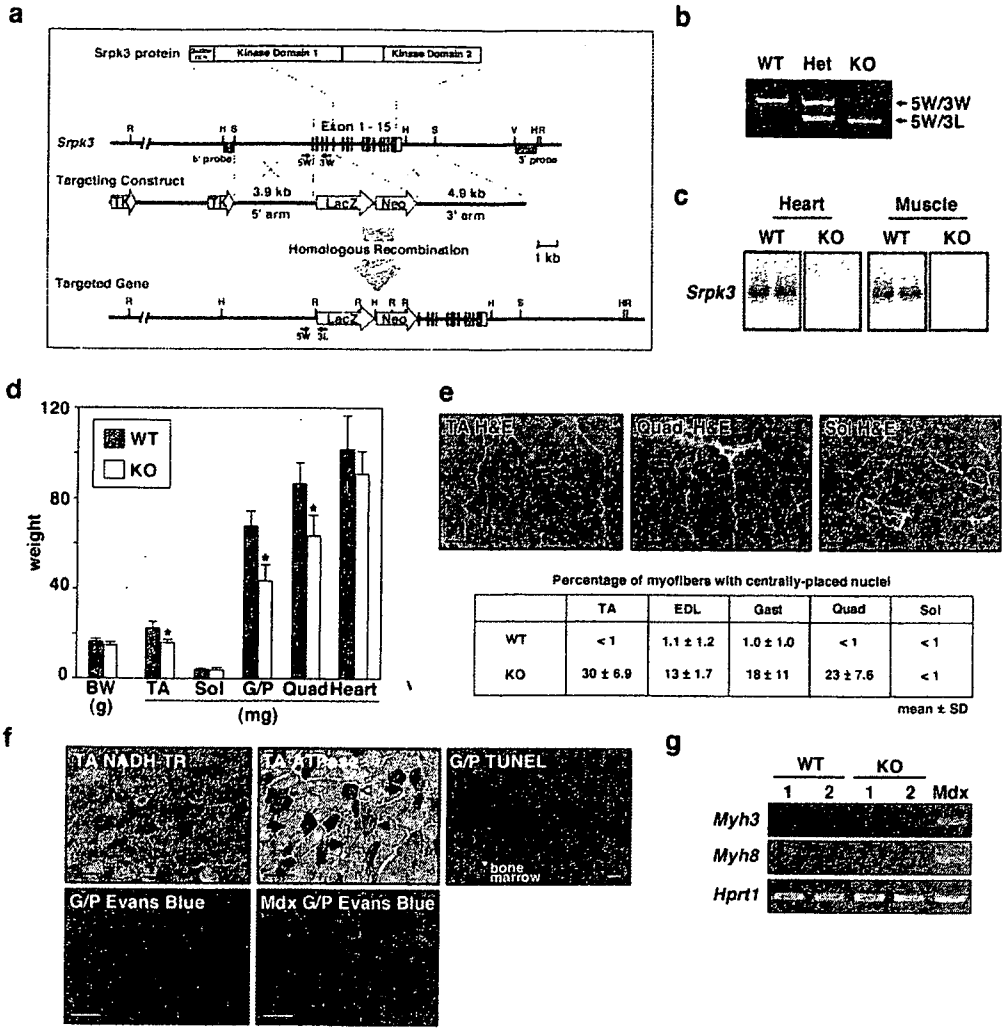

Figure 6. Centronuclear myopathy of *Srpk3*-null mice (*a*) Gene targeting strategy. The mouse *Srpk3* gene is shown with the targeting vector and the targeted allele. Parts of the exons 1 and 5, and the entire exons 2, 3, and 4 were replaced with the *LacZ–neomycin resistance* gene (*Neo*) cassette. Genotypes were determined by Southern blot analysis and PCR. The positions of the 5′ and 3′ Southern probes and PCR primers (5W, 3W, 3L) are shown. (TK) Thymidine kinase; (R) EcoRI; (H) HindIII; (S) SpeI; (V) EcoRV. (*b*) A representative result of PCR genotyping. (WT) Wild-type mouse; (Het) female heterozygous mouse; (KO) male hemizygously null mouse. (*c*) The *Srpk3* mRNA expression is not detectable in the heart and skeletal muscle of *Srpk3*-null mice by Northern blot analysis. (*d*) The weight of various skeletal muscle groups significantly decreased in *Srpk3*-null mice. (BW) Body weight. Mean ± SD; $n = 6$; (*) $p < 0.01$. (*E*) H&E staining of various muscle groups of *Srpk3*-null mice. Bars, 100 µm. Percentages of centrally placed nuclei are also shown ($n = 400$–600). (*f*) The NADH-TR, ATPase and TUNEL staining, and the result of Evans Blue injection of *Srpk3*-null mice. ATPase activity stains type 1 fibers dark blue (open triangle), type 2B fibers blue (filled triangle), and type 2A fibers light blue (arrows). Cells in the bone marrow, but not skeletal myocytes, showed positive signals in TUNEL staining. Evans Blue injection showed no apparent abnormality of sarcolemmal integrity in *Srpk3*-null mice, in contrast to Mdx dystrophic mice shown as a positive control. Bar, 100 µm. Muscle groups: (EDL) extensor digitorum longus; (G/P) gastrocnemius and plantaris; (Quad) quadriceps; (Sol) soleus; (TA) tibialis anterior. (*g*) Expression of muscle regeneration markers, *Myh3* and *Myh8*, is not activated in *Srpk3*-null mice, in contrast to Mdx mice. RT–PCR analysis.

muscle causes severe myofiber abnormalities, while overexpression in the heart results in dilated cardiomyopathy characterized by chamber dilatation, reduced contractility, and disease marker expression (M. Arnold, M. Nakagawa, H. Hamada, O. Nakagawa, J.A. Richardson, and E.N. Olson, unpubl.). Conversely, targeted deletion of the *Srpk3* gene results in a unique form of skeletal myopathy with a marked increase in centrally placed nuclei. The histological characteristics of these mice share similarity with those in human centronuclear myopathy, a congenital myopathy characterized by the presence of numerous centronuclear myofibers (Laporte et al. 1996; Carpenter and Karpati 2001; Jeannet et al. 2004).

Central placement of myonuclei occurs in various pathological conditions and commonly accompanies the regeneration process following myofiber degeneration and death (Garry et al. 2000; Carpenter and Karpati 2001; Emery 2002). In response to muscle injury, quiescent muscle progenitor cells, called satellite cells, are acti-

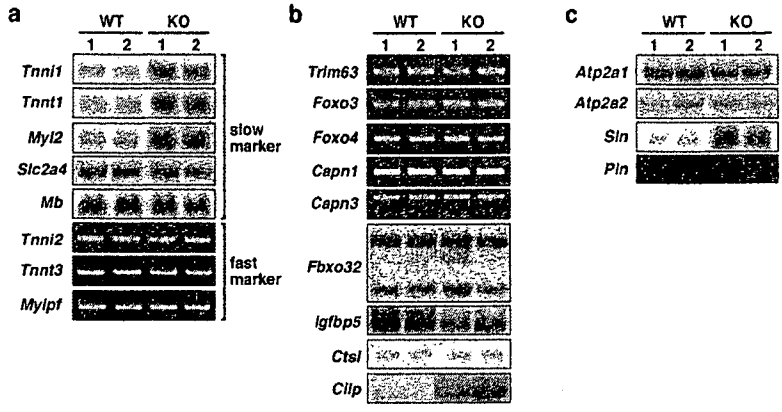

Figure 7. Expression profiles of muscle genes in *Srpk3*-null mice Expression of various muscle genes in the tibialis anterior muscle of *Srpk3*-null mice (KO) and wild-type control (WT). Ethidium bromide staining of RT–PCR products or phosphorimages of Northern blot hybridization are shown. (*a*) Slow- and fast-twitch myofiber markers. (*b*) Atrophy-related proteins. (*c*) Molecules related to calcium handling. At least three mice for each genotype were examined, and two representative results are shown. Gene names: (Atp2a1) ATPase, Ca^{++} transporting, cardiac muscle, fast twitch 1 or Serca1; (Atp2a2) ATPase, Ca^{++} transporting, cardiac muscle, slow twitch 2 or Serca2; (Capn1/-3) Calpain 1/-3; (Cilp), cartilage intermediate layer protein; (Ctsl) Cathepsin L; (Fbxo32) F-box-only protein 32, MAFbx or Atrogin-1; (Foxo3/-4) Forkhead box o3/o4; (Igfbp5) insulin-like growth factor-binding protein 5; (Mb) myoglobin; (Myl2) myosin, light polypeptide 2, regulatory, cardiac, slow; (Mylpf) myosin light chain, phosphorylatable, fast skeletal muscle; (Pln) Phospholamban; (Slc2a4) solute carrier family 2 (facilitated glucose transporter), member 4 or Glut4; (Sln) sarcolipin; (Tnni1) Troponin I, skeletal, slow 1; (Tnni2) Troponin I, skeletal, fast 2; (Tnnt1) Troponin T1, skeletal, slow; (Tnnt3) Troponin T3, skeletal, fast; (Trim63) tripartite motif-containing 63 or MuRF1.

vated and differentiate into new myofibers with centrally placed nuclei as are also seen in newly formed muscle fibers during embryonic development. However, in contrast to muscular dystrophy models, *Srpk3*-null mice did not show histological signs of myocyte death or reactivation of early developmental markers, which typically accompanies regeneration. Instead, the skeletal muscle of *Srpk3*-null mice may retain partially immature characteristics, although myofiber differentiation in these mice apparently progresses beyond the stages with embryonic and perinatal myosin expression. The conclusion that centronuclear myopathy in *Srpk3* mutant mice reflects a developmental abnormality is also supported by the absence of signs of muscle degeneration and regeneration, such as muscle cell death, myofiber disarray, or neutrophil infiltration, at early ages (data not shown).

The only gene shown to be involved in human centronuclear myopathy is *myotubularin 1* (*MTM1*), which encodes a ubiquitously expressed dual-specificity phosphatase (Laporte et al. 1996, 2003; Buj-Bello et al. 2002). Mutations of *MTM1* cause an X-linked form of centronuclear myopathy, characterized by an immature myotube-like appearance of skeletal muscle (Carpenter and Karpati 2001; Laporte et al. 2003). Null mutation of the *Mtm1* gene also causes centronuclear myopathy in mice (Buj-Bello et al. 2002). Muscle growth defects in *Mtm1*-null mice are more severe than those of *Srpk3*-null mice, and centrally placed nuclei are observed predominantly in type 1 fibers. However, these two models share similar features, such as the proportions of centronuclear myofibers and the lack of inflammation, apoptosis, and sarcolemmal disruption. The Myotubularin substrates that are related to skeletal muscle abnormalities remain unidentified. Perhaps there is cross-talk of signaling pathways downstream of Srpk3 and Myotubularin. The phenotype of *Srpk3* null mice also raises the question whether mutations in the *SRPK3* gene might be responsible for human myopathies that have not yet been ascribed to a specific gene.

Cellular functions of SRPK in skeletal muscle

The SRPK family of protein kinases is highly conserved among species; Sky1p and Dsk1 in yeast, SPK-1 in *C. elegans*, SRPK in *Drosophila*, and Srpk1 and Srpk2 in mice and humans (Gui et al. 1994; Bedford et al. 1997; Kuroyanagi et al. 1998, 2000; Tang et al. 1998; Wang et al. 1998; Siebel et al. 1999). SRPKs phosphorylate serine/arginine (SR)-rich domain proteins and modulate their protein–protein interactions and intracellular localization. For example, unphosphorylated SR splicing factors associate with SRPK in the cytoplasm and, once phosphorylated, dissociate from SRPK and are translocated to the nucleus (Koizumi et al. 1999; Yeakley et al. 1999).

In this regard, it is interesting to note that abnormal mRNA splicing has been implicated in a variety of muscle diseases (Maniatis and Tasic 2002), and cardiac-specific deletion of the SR splicing factor genes, *Sfrs1* and *Sfrs2*, causes dilated cardiomyopathy in mice (Ding et al. 2004; Xu et al. 2005). Additionally, splicing defects of the tyrosine phosphatase-like gene, *Ptpla*, lead to centronuclear myopathy in dogs (Pele et al. 2005). SRPKs also phosphorylate Lamin B Receptor, an integral protein in the inner nuclear membrane or nuclear lamina (Nikolakaki et al. 1997; Ye et al. 1997; Takano et al. 2002). Mutations of the genes encoding the nuclear lamina proteins, Emerin or Lamin A/C, cause Emery-Dreifuss type muscular dystrophy (Wilson 2000). Thus, it is tempting to speculate that defects of mRNA splicing or nuclear lamina assembly contribute to the muscle abnormalities in *Srpk3*-null and *Srpk3* transgenic mice.

It should also be pointed out that proteins without typical SR-rich domains have recently been shown to serve as SRPK substrates (Daub et al. 2002). Although *Srpk3* expression is equivalent in type 1- and type 2-enriched muscles (data not shown), there is apparent fiber type specificity of the muscle pathology in *Srpk3*-null mice, suggesting the involvement of Srpk3 in muscle functions that are important in type 2 fibers, such as

glycolytic metabolism. The abnormal muscle gene expression profiles of *Srpk3*-null mice suggest roles of Srpk3 in growth factor signaling and calcium homeostasis. Identification of muscle-enriched SRPK substrates will provide further insights into functions of Srpk3 in muscle development and disease.

MEF2 as a nexus of kinase signaling pathways

A variety of kinase signaling pathways have been shown to augment MEF2 activity (McKinsey et al. 2002). Signaling by p38 MAP kinase, for example, results in phosphorylation of the transcription activation domain of MEF2 and consequent enhancement of transcriptional activity (Han et al. 1997), while the MAP kinase ERK5 interacts directly with MEF2 and serves as a transcriptional coactivator (Kato et al. 1997; Yang et al. 1998; Kasler et al. 2000). In addition, signaling by calcium/calmodulin-dependent kinase and protein kinases C and D induces MEF2 activity by releasing the repressive influence imposed by class II histone deacetylases (McKinsey et al. 2000; Vega et al. 2004). The results of this study, which show that MEF2 is an obligate activator of *Srpk3* expression, point to MEF2 as a nexus between upstream and downstream kinase signaling pathways that control muscle development and function.

Materials and methods

Mef2c-*null embryos, microarray analysis, and cloning of Srpk3 cDNA*

Since *Mef2c*-null embryos die around E9.5 (Lin et al. 1997), the hearts from the wild-type and *Mef2c*-null embryos were collected prior to overt cardiac demise at E9.0. Microarray analysis was performed using 1 μg of total RNA as previously described (Belbin et al. 2002). The data were queried for difference of signal intensity between two samples, reproducibility in dye swap arrays, and signal intensity compared with local background. A clone that showed decreased signals in the hybridization with *Mef2c*-null embryo-derived RNA probes was identical to a part of mouse *Stk23/Srpk3* cDNA sequence (NM_019684). Full-length *Srpk3* cDNA fragments were isolated by screening of an embryonic heart cDNA library (Stratagene), using partial cDNA fragments obtained from the EST resources as a probe. Full-length cDNA fragments of human *SRPK3* were also obtained from the EST resources.

Cell culture

C2C12 myoblasts were maintained in the growth medium containing 10% fetal calf serum, and the plasmid transfection was performed using Lipofectamine (Invitrogen) according to the manufacturer's instructions. Myogenic differentiation of C2C12 cells was triggered by the transfer to the differentiation medium containing 2% horse serum (Lu et al. 2000). For the luciferase assays during the course of differentiation, C2C12 cells were transfected with the plasmids in growth medium, and myogenic differentiation was stimulated 2 d after the transfection.

Srpk3 transgenic mice

Transgenic mice overexpressing Flag-tagged Srpk3 were generated using the *MCK* promoter/enhancer (Sternberg et al. 1988). Genotyping was performed by Southern blot analysis, and the skeletal muscle-specific expression of Flag-Srpk3 was confirmed by Western blot analysis.

Srpk3-*null mice*

A BAC clone containing the *Srpk3* gene was obtained by screening of a 129s6/SvEvTAC mouse genomic BAC library (BACPAC Resources). The targeting vector was linearized and electroporated into mouse embryonic stem cells of 129Sv origin. Correctly targeted embryonic stem cell clones, as identified by Southern blotting using both 5′ and 3′ probes, were injected into blastocysts isolated from C57BL/J mice. Chimeras obtained from these blastocyst injections were bred to obtain heterozygous mice that carry the targeted *Srpk3* locus in their germline. Genotyping was performed by Southern blot analysis and PCR (primers: 5W, 5′-AGGTCTTCCTTGGCTAGTCCTACACTGTGG-3′; 3W, 5′-TAGTCCTTAGGGTCTTCCTGTTCCTCATC-3′; and 3L, 5′-CCATGGTGGATCCTGAGACTGGGGAATTC-3′). *Srpk3*-null mice in the pure 129s6/SvEvTAC background and the mixed 129s6/SvEvTAC-C57BL6/J background showed identical skeletal muscle pathology.

In situ hybridization

Whole-mount and radioactive section in situ hybridization was performed as described (Nakagawa et al. 1999), using *Srpk1/-2/-3* RNA probes. For each gene, identical results were obtained using two probes that were prepared using different cDNA fragments.

Northern blot analysis

Northern blot analysis of the SRPK family genes was performed on mouse and human poly(A)$^+$ RNA blots (Clontech), as described (Nakagawa et al. 1999). Northern blot analysis of muscle genes was performed using total RNA of the tibialis anterior muscle of *Srpk3*-null and wild-type mice. cDNA fragments for probe preparation were prepared by RT–PCR or were obtained from the EST resources. Detailed information of the cDNA probes is available upon request.

RT–PCR

RT–PCR was performed using Superscript II reverse transcriptase (Invitrogen) and Advantage2 DNA polymerase (Clontech). Primer sequences are available upon request.

Luciferase and LacZ reporter analyses

Three different *Srpk3* genomic DNA fragments, which had the identical 3′-ends at the translational start site, were ligated into a luciferase reporter plasmid, pGL3 basic (Promega). The genomic DNA fragments were also ligated into a promoter-less *LacZ* reporter plasmid or a *LacZ* reporter plasmid containing the *HSP68* minimal promoter sequence (Wang et al. 2001). Mutations were introduced by PCR into a MEF2-binding site (wild-type, 5′-GGCTATTTATAAAG-3′; mutant, 5′-GGCTAGGGCTAAAG-3′) and E boxes (wild-type, 5′-CAGCTG-3′; mutant, 5′-ACGCGT-3′) in the *Srpk3* regulatory region of the reporter plasmids. Luciferase assays were performed in C2C12 cells, and *LacZ* reporter assays of F0 transgenic mouse embryos were per-

formed as previously described (Nakagawa et al. 2000; Wang et al. 2001).

Electrophoretic mobility shift assay

The cell lysates containing MEF2C, myogenin, and/or E12 were prepared from COS1 cells transfected with combinations of expression plasmids. In vitro binding analysis was performed as previously described (Wang et al. 2001), using oligonucleotide fragments that contained a MEF2-binding site and E boxes (underlined) in the *Srpk3* promoter (5′-CTTGCCCACAGCTGAG CAGCTGGGAGGCTATTTATAAAGGCGAG-3′). The oligonucleotide fragments with a mutated MEF2-binding site (5′-GGCTAGGGCTAAAG-3′) and those with mutated E boxes (5′-ACGCGT-3′) did not show binding by MEF2C and the myogenin/E12 complex, respectively (data not shown).

In vitro phosphorylation assays

Myc-tagged proteins of full-length SF2/ASF (Koizumi et al. 1999) and the N terminus of Lamin B Receptor (Ye et al. 1997) were prepared by in vitro transcription and translation using TNT reticulocyte lysate system (Promega). Myc-Srpk3 and the control sample prepared using the empty plasmid vector were also prepared by the TNT reaction. Proteins were immunoprecipitated using rabbit polyclonal anti-Myc antibody (Santa Cruz), and in vitro kinase reaction was performed with [γ-^{32}P]ATP at 30°C.

Histological analysis of skeletal muscle

Histological staining of skeletal muscles, myofiber typing by the ATPase staining, TUNEL staining, and the Evans Blue dye injection were performed as previously described (Woods and Ellis 1996; Wu et al. 2000; Lu et al. 2002; Kanagawa et al. 2004).

Acknowledgments

We thank M. Hagiwara and H. Worman for plasmids; J. Hill, K. Kamm, M. Bennett, L. Leinwand, Y.K. Hayashi, K. Murayama, D. Garry, and R. Bassel-Duby for discussion; and J. McAnally, C. Nolan, J. Bartos, and J. Fields for technical assistance. O.N. was supported by a grant from the Muscular Dystrophy Association. E.N.O. was supported by grants from the NIH, the Donald W. Reynolds Center for Clinical Cardiovascular Research, the Robert A. Welch Foundation, and the Muscular Dystrophy Association. G.C. and T.M.M. were supported by an NIH grant (NIH HL083488). M.A. was supported by the Medical Scientist Training Program at University of Texas Southwestern and NIH T-32-GM08014.

References

Anderson, J.P., Dodou, E., Heidt, A.B., De Val, S.J., Jaehnig, E.J., Greene, S.B., Olson, E.N., and Black, B.L. 2004. HRC is a direct transcriptional target of MEF2 during cardiac, skeletal, and arterial smooth muscle development in vivo. *Mol. Cell. Biol.* **24:** 3757–3768.

Bailey, P., Holowacz, T., and Lassar, A.B. 2001. The origin of skeletal muscle stem cells in the embryo and the adult. *Curr. Opin. Cell Biol.* **13:** 679–689.

Bedford, M.T, Chan, D.C., and Leder, P. 1997. FBP WW domains and the Abl SH3 domain bind to a specific class of proline-rich ligands. *EMBO J.* **16:** 2376–2383.

Belbin, T., Singh, B., Barber, I., Socci, N., Wenig, B., Smith, R., Prystowsky, M., and Childs, G. 2002. Molecular classification of head and neck squamous cell carcinoma using cDNA microarrays. *Cancer Res.* **62:** 1184–1190.

Black, B.L. and Olson, E.N. 1998. Transcriptional control of muscle development by myocyte enhancer factor-2 (MEF2) proteins. *Annu. Rev. Cell Dev. Biol.* **14:** 167–196.

Blais, A., Tsikitis, M., Acosta-Alvear, D., Sharan, R., Kluger, Y., and Dynlacht, B.D. 2005. An initial blueprint for myogenic differentiation. *Genes & Dev.* **19:** 553–569.

Bour, B.A., O'Brien, M.A., Lockwood, W.L., Goldstein, E.S., Bodmer, R., Taghert, P.H., Abmayr, S.M., and Nguyen, H.T. 1995. *Drosophila* MEF2, a transcription factor that is essential for myogenesis. *Genes & Dev.* **9:** 730–741.

Buckingham, M., Bajard, L., Chang, T., Daubas, P., Hadchouel, J., Meilhac, S., Montarras, D., Rocancourt, D., and Relaix, F. 2003. The formation of skeletal muscle: From somite to limb. *J. Anat.* **202:** 59–68.

Buj-Bello, A., Laugel, V., Messaddeq, N., Zahreddine, H., Laporte, J., Pellissier, J.F., and Mandel, J.L. 2002. The lipid phosphatase myotubularin is essential for skeletal muscle maintenance but not for myogenesis in mice. *Proc. Natl. Acad. Sci.* **99:** 15060–15065.

Carpenter, S. and Karpati, G., 2001. *Pathology of skeletal muscle.* Oxford University Press, New York.

Cheng, T.C., Wallace, M.C., Merlie, J.P., and Olson, E.N. 1993. Separable regulatory elements governing myogenin transcription in mouse embryogenesis. *Science* **261:** 215–218.

Cserjesi, P. and Olson, E.N. 1991. Myogenin induces the myocyte-specific enhancer binding factor MEF-2 independently of other muscle-specific gene products. *Mol. Cell. Biol.* **11:** 4854–4862.

Daub, H., Blencke, S., Habenberger, P., Kurtenbach, A., Dennenmoser, J., Wissing, J., Ullrich, A., and Cotton, M. 2002. Identification of SRPK1 and SRPK2 as the major cellular protein kinases phosphorylating hepatitis B virus core protein. *J. Virol.* **76:** 8124–8137.

Ding, J.H., Xu, X., Yang, D., Chu, P.H., Dalton, N.D., Ye, Z., Yeakley, J.M., Cheng, H., Xiao, R.P., Ross, J., et al. 2004. Dilated cardiomyopathy caused by tissue-specific ablation of SC35 in the heart. *EMBO J.* **23:** 885–896.

Dodou, E., Xu, S.M., and Black, B.L. 2003. Mef2c is activated directly by myogenic basic helix–loop–helix proteins during skeletal muscle development in vivo. *Mech. Dev.* **120:** 1021–1032.

Edmondson, D.G., Cheng, T.-C., Cserjesi, P., Chakraborty, T., and Olson, E.N. 1992. Analysis of the myogenin promoter reveals an indirect pathway for positive autoregulation mediated by the muscle-specific enhancer factor MEF-2. *Mol. Cell. Biol.* **12:** 3665–3677.

Emery, A.E. 2002. The muscular dystrophies. *Lancet* **359:** 687–695.

Garry, D.J., Meeson, A., Elterman, J., Zhao, Y., Yang, P., Bassel-Duby, R., and Williams, R.S. 2000. Myogenic stem cell function is impaired in mice lacking the forkhead/winged helix protein MNF. *Proc. Natl. Acad. Sci.* **97:** 5416–5421.

Grunau, C., Hindermann, W., and Rosenthal, A. 2000. Large-scale methylation analysis of human genomic DNA reveals tissue-specific differences between the methylation profiles of genes and pseudogenes. *Hum. Mol. Genet.* **9:** 2651–2663.

Gui, J.F., Lane, W.S., and Fu, X.D. 1994. A serine kinase regulates intracellular localization of splicing factors in the cell cycle. *Nature* **369:** 678–682.

Han, J., Jiang, Y., Li, Z., Kravchenko, V.V., and Ulevitch, R.J. 1997. Activation of the transcription factor MEF2C by the MAP kinase p38 in inflammation. *Nature* **386:** 296–299.

Jeannet, P.Y., Bassez, G., Eymard, B., Laforet, P., Urtizberea, J.A., Rouche, A., Guicheney, P., Fardeau, M., and Romero,

N.B. 2004. Clinical and histologic findings in autosomal centronuclear myopathy. *Neurology* **62:** 1484–1490.

Johnson, K., Farley, D., Hu, S.I., and Terkeltaub, R. 2003. One of two chondrocyte-expressed isoforms of cartilage intermediate-layer protein functions as an insulin-like growth factor 1 antagonist. *Arthritis Rheum.* **48:** 1302–1314.

Kanagawa, M., Saito, F., Kunz, S., Yoshida-Moriguchi, T., Barresi, R., Kobayashi, Y.M., Muschler, J., Dumanski, J.P., Michele, D.E., Oldstone, M.B., et al. 2004. Molecular recognition by LARGE is essential for expression of functional dystroglycan. *Cell* **117:** 953–964.

Kasler, H.G., Victoria, J., Duramad, O., and Winoto, A. 2000. ERK5 is a novel type of mitogen-activated protein kinase containing a transcriptional activation domain. *Mol. Cell. Biol.* **20:** 8382–8389.

Kato, Y., Kravchenko, V.V., Tapping, R.I., Han, J., Ulevitch, R.J., and Lee, J.D. 1997. BMK1/ERK5 regulates serum-induced early gene expression through transcription factor MEF2C. *EMBO J.* **16:** 7054–7066.

Koizumi, J., Okamoto, Y., Onogi, H., Mayeda, A., Krainer, A.R., and Hagiwara, M. 1999. The subcellular localization of SF2/ASF is regulated by direct interaction with SR protein kinases (SRPKs). *J. Biol. Chem.* **274:** 11125–11131.

Kuisk, I.R., Li, H., Tran, D., and Capetanaki, Y. 1996. A single MEF2 site governs desmin transcription in both heart and skeletal muscle during mouse embryogenesis. *Dev. Biol.* **174:** 1–13.

Kuroyanagi, N., Onogi, H., Wakabayashi, T., and Hagiwara, M. 1998. Novel SR-protein-specific kinase, SRPK2, disassembles nuclear speckles. *Biochem. Biophys. Res. Commun.* **242:** 357–364.

Kuroyanagi, H., Kimura, T., Wada, K., Hisamoto, N., Matsumoto, K., and Hagiwara, M. 2000. SPK-1, a *C. elegans* SR protein kinase homologue, is essential for embryogenesis and required for germline development. *Mech. Dev.* **99:** 51–64.

Laporte, J., Hu, L.J., Kretz, C., Mandel, J.L., Kioschis, P., Coy, J.F., Klauck, S.M., Poustka, A., and Dahl, N. 1996. A gene mutated in X-linked myotubular myopathy defines a new putative tyrosine phosphatase family conserved in yeast. *Nat. Genet.* **13:** 175–182.

Laporte, J., Bedez, F., Bolino, A., and Mandel, J.L. 2003. Myotubularins, a large disease-associated family of cooperating catalytically active and inactive phosphoinositides phosphatases. *Hum. Mol. Genet.* **12 Spec No 2:** R285–R292.

Lassar, A.B., Davis, R.L., Wright, W.E., Kadesch, T., Murre, C., Voronova, A., Baltimore, D., and Weintraub, H. 1991. Functional activity of myogenic HLH proteins requires hetero-oligomerization with E12/E47-like proteins in vivo. *Cell* **66:** 305–315.

Lilly, B., Zhao, B., Ranganayakulu, G., Paterson, B.M., Schulz, R.A., and Olson, E.N. 1995. Requirement of MADS domain transcription factor D-MEF2 for muscle formation in *Drosophila*. *Science* **267:** 688–693.

Lin, Q., Schwarz, J., Bucana, C., and Olson, E.N. 1997. Control of mouse cardiac morphogenesis and myogenesis by transcription factor MEF2C. *Science* **276:** 1404–1407.

Lorenzo, P., Bayliss, M.T., and Heinegard, D. 1998. A novel cartilage protein (CILP) present in the mid-zone of human articular cartilage increases with age. *J. Biol. Chem.* **273:** 23463–23468.

Lu, J., McKinsey, T.A., Zhang, C.L., and Olson, E.N. 2000. Regulation of skeletal myogenesis by association of the MEF2 transcription factor with class II histone deacetylases. *Mol. Cell* **6:** 233–244.

Lu, J.R., Bassel-Duby, R., Hawkins, A., Chang, P., Valdez, R., Wu, H., Gan, L., Shelton, J.M., Richardson, J.A., and Olson, E.N. 2002. Control of facial muscle development by MyoR and capsulin. *Science* **298:** 2378–2381.

MacLennan, D.H., Asahi, M., and Tupling, A.R. 2003. The regulation of SERCA-type pumps by phospholamban and sarcolipin. *Ann. NY Acad. Sci.* **986:** 472–480.

Maniatis, T. and Tasic, B. 2002. Alternative pre-mRNA splicing and proteome expansion in metazoans. *Nature* **418:** 236–243.

McCullagh, K.J., Calabria, E., Pallafacchina, G., Ciciliot, S., Serrano, A.L., Argentini, C., Kalhovde, J.M., Lomo, T., and Schiaffino, S. 2004. NFAT is a nerve activity sensor in skeletal muscle and controls activity-dependent myosin switching. *Proc. Natl. Acad. Sci.* **101:** 10590–10595.

McKinnell, I.W. and Rudnicki, M.A. 2004. Molecular mechanisms of muscle atrophy. *Cell* **119:** 907–910.

McKinsey, T.A., Zhang, C.L., Lu, J., and Olson, E.N. 2000. Signal-dependent nuclear export of a histone deacetylase regulates muscle differentiation. *Nature* **408:** 106–111.

McKinsey, T.A., Zhang, C.L., and Olson, E.N. 2002. Signaling chromatin to make muscle. *Curr. Opin. Cell Biol.* **14:** 763–772.

Nakagawa, O., Nakagawa, M., Richardson, J.A., Olson, E.N., and Srivastava, D. 1999. HRT1, HRT2, HRT3: A new subclass of bHLH transcription factors marking specific cardiac, somitic and pharyngeal arch segments. *Dev. Biol.* **216:** 72–84.

Nakagawa, O., McFadden, D.G., Nakagawa, M., Yanagisawa, H., Hu, T., Srivastava, D., and Olson, E.N. 2000. Members of the HRT family of bHLH proteins act as transcriptional repressors downstream of Notch signaling. *Proc. Natl. Acad. Sci.* **97:** 13655–13660.

Nikolakaki, E., Meier, J., Simos, G., Georgatos, S.D., and Giannakouros, T. 1997. Mitotic phosphorylation of the Lamin B Receptor by a serine/arginine kinase and p34(cdc2). *J. Biol. Chem.* **272:** 6208–6213.

Parker, M.H., Seale, P., and Rudnicki, M.A. 2003. Looking back to the embryo: Defining transcriptional networks in adult myogenesis. *Nat. Rev. Genet.* **4:** 497–507.

Pele, M., Tiret, L., Kessler, J.L., Blot, S., and Panthier, J.J. 2005. A SINE exonic insertion in the PTPLA gene leads to multiple splicing defects and segregates with the autosomal recessive centronuclear myopathy in dog. *Hum. Mol. Genet.* **14:** 1417–1427.

Phan, D., Rasmussen, T.L., Nakagawa, O., McAnally, J., Gottlieb, P.D., Tucker, P.W., Richardson, J.A., Bassel-Duby, R., and Olson, E.N. 2005. *Bop*, a regulator of right ventricular heart development, is a direct transcriptional target of MEF2C in the anterior heart field. *Development* **132:** 2669–2678.

Pownall, M.E., Gustafsson, M.K., and Emerson Jr., C.P. 2002. Myogenic regulatory factors and the specification of muscle progenitors in vertebrate embryos. *Annu. Rev. Cell Dev. Biol.* **18:** 747–783.

Seki, S., Kawaguchi, Y., Chiba, K., Mikami, Y., Kizawa, H., Oya, T., Mio, F., Mori, M., Miyamoto, Y., Masuda, I., et al. 2005. A functional SNP in *CILP*, encoding cartilage intermediate layer protein, is associated with susceptibility to lumbar disc disease. *Nat. Genet.* **37:** 607–612.

Serrano, A.L., Murgia, M., Pallafacchina, G., Calabria, E., Coniglio, P., Lomo, T., and Schiaffino, S. 2001. Calcineurin controls nerve activity-dependent specification of slow skeletal muscle fibers but not muscle growth. *Proc. Natl. Acad. Sci.* **98:** 13108–13113.

Siebel, C.W., Feng, L., Guthrie, C., and Fu, X.D. 1999. Conservation in budding yeast of a kinase specific for SR splicing

factors. *Proc. Natl. Acad. Sci.* **96:** 5440–5445.
Sternberg, E.A., Spizz, G., Perry, W.M., Vizard, D., Weil, T., and Olson, E.N. 1988. Identification of upstream and intragenic regulatory elements that confer cell-type-restricted and differentiation-specific expression on the muscle creatine kinase gene. *Mol. Cell. Biol.* **8:** 2896–2909.
Takano, M., Takeuchi, M., Ito, H., Furukawa, K., Sugimoto, K., Omata, S., and Horigome, T. 2002. The binding of lamin B receptor to chromatin is regulated by phosphorylation in the RS region. *Eur. J. Biochem.* **269:** 943–953.
Tang, Z., Yanagida, M., and Lin, R.J. 1998. Fission yeast mitotic regulator Dsk1 is an SR protein-specific kinase. *J. Biol. Chem.* **273:** 5963–5969.
Teboul, L., Hadchouel, J., Daubas, P., Summerbell, D., Buckingham, M., and Rigby, P.W. 2002. The early epaxial enhancer is essential for the initial expression of the skeletal muscle determination gene Myf5 but not for subsequent, multiple phases of somitic myogenesis. *Development* **129:** 4571–4580.
Tupling, A.R., Asahi, M., and MacLennan, D.H. 2002. Sarcolipin overexpression in rat slow twitch muscle inhibits sarcoplasmic reticulum Ca^{2+} uptake and impairs contractile function. *J. Biol. Chem.* **277:** 44740–44746.
Vega, R.B., Harrison, B.C., Meadows, E., Roberts, C.R., Papst, P.J., Olson, E.N., and McKinsey, T.A. 2004. Protein kinases C and D mediate agonist-dependent cardiac hypertrophy through nuclear export of histone deacetylase 5. *Mol. Cell. Biol.* **24:** 8374–8385.
Wang, H.Y., Lin, W., Dyck, J.A., Yeakley, J.M., Songyang, Z., Cantley, L.C., and Fu, X.D. 1998. SRPK2: A differentially expressed SR protein-specific kinase involved in mediating the interaction and localization of pre-mRNA splicing factors in mammalian cells. *J. Cell Biol.* **140:** 737–750.
Wang, D.Z., Valdez, M.R., McAnally, J., Richardson, J., and Olson, E.N. 2001. The Mef2c gene is a direct transcriptional target of myogenic bHLH and MEF2 proteins during skeletal muscle development. *Development* **128:** 4623–4633.
Wilson, K.L. 2000. The nuclear envelope, muscular dystrophy and gene expression. *Trends Cell Biol.* **10:** 125–129.
Woods, A.E. and Ellis, R.C. 1996. *Laboratory histopathology, a complete reference.* Churchill-Livingston Press, Oxford.
Wu, H., Naya, F.J., McKinsey, T.A., Mercer, B., Shelton, J.M., Chin, E.R., Simard, A.R., Michel, R.N., Bassel-Duby, R., Olson, E.N., et al. 2000. MEF2 responds to multiple calcium-regulated signals in the control of skeletal muscle fiber type. *EMBO J.* **19:** 1963–1973.
Xu, X., Yang, D., Ding, J.H., Wang, W., Chu, P.H., Dalton, N.D., Wang, H.Y., Bermingham Jr., J.R., Ye, Z., Liu, F., et al. 2005. ASF/SF2-regulated CaMKIIδ alternative splicing temporally reprograms excitation–contraction coupling in cardiac muscle. *Cell* **120:** 59–72.
Yang, C.C., Ornatsky, O.I., McDermott, J.C., Cruz, T.F., and Prody, C.A. 1998. Interaction of myocyte enhancer factor 2 (MEF2) with a mitogen-activated protein kinase, ERK5/BMK1. *Nucleic Acids Res.* **26:** 4771–4777.
Ye, Q., Callebaut, I., Pezhman, A., Courvalin, J.C., and Worman, H.J. 1997. Domain-specific interactions of human HP1-type chromodomain proteins and inner nuclear membrane protein LBR. *J. Biol. Chem.* **272:** 14983–14989.
Yeakley, J.M., Tronchere, H., Olesen, J., Dyck, J.A., Wang, H.Y., and Fu, X.D. 1999. Phosphorylation regulates in vivo interaction and molecular targeting of serine/arginine-rich pre-mRNA splicing factors. *J. Cell Biol.* **145:** 447–455.
Yee, S.P. and Rigby, P.W. 1993. The regulation of myogenin gene expression during the embryonic development of the mouse. *Genes & Dev.* **7:** 1277–1289.

Gene expression analyses in X-linked myotubular myopathy

S. Noguchi, PhD; M. Fujita, MSc; K. Murayama, BSc; R. Kurokawa, MSc; and I. Nishino, MD, PhD

Abstract—*Background:* X-linked myotubular myopathy (XLMTM) is a severe congenital disorder characterized by marked muscle weakness and hypotonia. Myotubularin, the protein product of the causative gene, *MTM1*, is thought to be a phosphatase for phosphatidylinositol-3-phosphate and may be involved in membrane trafficking. Analysis of MTM1 knocked-out mice indicates that the characteristic small fibers in XLMTM muscles are due to atrophy rather than hypoplasia. *Objective:* To characterize gene expression profiling of skeletal muscles with XLMTM. *Method:* The authors analyzed the expression of more than 4,200 genes in skeletal muscles from eight patients with XLMTM using their custom cDNA microarray. *Results:* In XLMTM, gene expression analysis revealed pathognomonic upregulation of transcripts for cytoskeletal and extracellular matrix proteins within or around atrophic myofibers. *Conclusion:* Remodeling of cytoskeletal and extracellular architecture appears to contribute to atrophy and intracellular organelle disorganization in XLMTM myofibers.

NEUROLOGY 2005;65:732–737

X-linked myotubular myopathy (XLMTM; OMIM 310400) is a severe congenital disease characterized by marked muscle weakness, hypotonia, and feeding and breathing difficulties in male infants.[1] Most XLMTM patients die during the first year of life due to respiratory insufficiency.[2] The responsible gene for XLMTM, *MTM1*, has been identified by positional cloning.[3] Approximately 200 different mutations in this gene have been identified.[4-7]

XLMTM muscle has uniform histopathologic features, with small rounded myofibers that are predominantly type 1, centrally located myonuclei, and accumulations of mitochondria in peripheral halos.[8] Since these features resemble those of fetal muscle or myotubes, XLMTM had been attributed to an arrest of myogenesis[9]; however, *MTM1* knockout mice revealed normal muscle differentiation and, at about age 4 weeks, the animals developed a generalized and progressive myopathy with amyotrophy and accumulations of centralized nuclei.[10] Therefore, myotubularin seems to be essential for skeletal muscle maintenance rather than myogenesis.

In vitro experiments indicate that myotubularin is a 3-phosphatase for phosphatidylinositol 3-monophosphate [PtdIns3P] and phosphatidylinositol 3,5-bisphosphates [PtdIns (3, 5)P2].[11,12] Myotubularin has been localized to Rac1-induced membrane ruffles and intracellular vesicles with the 3-phosphatase adaptor protein (3-PAP) in cultured cells.[13,14] Phosphoinositide 3-kinase-derived molecules regulate diverse signaling functions including vesicular trafficking, actin cytoskeletal rearrangement, apoptosis, and cell proliferation.[15,16] These facts suggest that myotubularin is involved in membrane trafficking[17]; nevertheless, the biologic function of myotubularin remains uncertain.

cDNA microarray is a powerful tool to monitor, at the molecular level, the pathophysiologic states of various muscle diseases through comprehensive analyses of transcriptional alterations.[18-21] These data have added new molecular information to classic pathologic analyses, provided insights into pathomechanism of the disorders, and allowed monitoring of the status of muscle. Congenital myopathies usually show relatively static pathologic features and the ages of patients at biopsy are comparable. Designing an experiment for the analyses based on statistical calculation like comprehensive gene analyses should be easy. However, only nemaline myopathy has been analyzed.[22] Here, we examined the expression of genes in skeletal muscles of genetically diagnosed XLMTM patients and determined the genes with expression alterations that are specific to XLMTM. We also characterized the expression of their gene products in skeletal muscles of XLMTM patients.

Additional material related to this article can be found on the *Neurology* Web site. Go to www.neurology.org and scroll down the Table of Contents for the September 13 issue to find the title link for this article.

From the Department of Neuromuscular Research, National Institute of Neuroscience, National Center of Neurology and Psychiatry (NCNP), Kodaira, Tokyo, Japan; and Core Research for Evolutional Science and Technology (CREST), Japan Science and Technology Corporation, Kawaguchi, Saitama, Japan.

Supported by the Research Grant (16B-2) for Nervous and Mental Disorders from the Ministry of Health, Labor and Welfare of Japan, and Research on Health Sciences focusing on Drug Innovation from The Japan Health Science Foundation.

Disclosure: The authors report no conflicts of interest.

Received February 1, 2005. Accepted in final form May 27, 2005.

Address correspondence and reprint requests to Dr. Satoru Noguchi, Department of Neuromuscular Research, National Institute of Neuroscience, National Center of Neurology and Psychiatry,4-1-1 Ogawahigashi, Kodaira, Tokyo, 187-8502, Japan; e-mail: noguchi@ncnp.go.jp

Table 1 List of patients with X-linked myotubular myopathy (XLMTM)

Patient	Age, mo	Mutation	Patient no. in ref. 23
1	7	c.1067G>A	5
2	2	c.664C>T	14
3	4	c.624C>t	2
4	2	c.109C>T	12
5	1	c.1433-1436delTCTT	29
6	5	c.528+1G>A	19
7	2	c.1456C>T	17
8	4	EX9del	30
9	1	c.1262C>T	16
10	9	c.1261-10A>G	23

Methods. *Patients.* The age at biopsy and the mutation of *MTM1* gene in each patient used in this study are shown in table 1. The clinical features of each patient were described previously.[23] Patient numbers used in this article in contrast to those in reference 23 are also shown in table 1.

Microarray hybridization and data analysis. The cDNA microarray with 5,760 probes of 4,200 genes that are expressed in skeletal muscle was developed from a prior version.[21] RNA extractions, hybridizations, and detection of hybridized probes were as described.[21] We filtered probe spots with intensity values more than $\chi+2\sigma$ (χ: average intensity of non-spotted areas, σ: its SD). The data of residual spots were analyzed by Genespring software 4.1 (Silicon Genetics, Redwood City, CA). By combining repeated experiments, we identified single-fold changes and significance values for data points common to multiple microarrays. Hierarchical analyses among individuals or disorders were performed with Pearson correlation.

General design of experiments. RNA was extracted from the fresh-frozen muscles of eight patients with *MTM1* mutation and six age-matched control individuals. Microarray analysis was hybridized competitively with Cy3-labeled cDNA probes from RNA from biopsied muscle and Cy5-labeled cDNA probes from commercially available RNA (Origene, Rochville, MD). For each specimen, one to three microarray experiments were carried. The gene expression data from other muscle disorders were used for the comparison as follows: Duchenne muscular dystrophy, 3 patients; limb-girdle muscular dystrophy type 1C, 2 patients; XLMTM, 8 patients; Fukuyama-type congenital muscular dystrophy, 5 patients; merosin-negative congenital muscular dystrophy, 2 patients; collagen VI-deficient congenital muscular dystrophy, 6 patients.

Quantitative RT-PCR. To measure the amounts of mRNA, we performed quantitative PCR with QuantiTect SYBR Green PCR kit (Qiagen GmbH, Hilden, Germany) by iCycler iQ real-time PCR detection system (Bio-Rad, Hercules, CA). We measured transcripts for osteonectin, gelsolin, and glyceraldehyde phosphate dehydrogenase (GAPDH) as controls to normalize transcription level among the specimen. Primer sequences used in this study are as follows: osteonectin primers F-gagacctgtgacctggacaatga, R-gatccttgtcgatatccttctgc, gelsolin primers F- tgtgcaggtggcagaaggcagcga, R-catccatattattgtccttcagc, GAPDH primers F-ggtaaagtggatattgttgccatcaatg, R-ggagggatctcgctcctggaagatggtg.

Immunohistochemical staining and Western blotting. Immunohistochemical staining and Western blotting of biopsed muscle specimens were performed as described previously.[24] We analyzed 10 μg of extracted proteins from muscles. The antibodies used in this study are mouse monoclonal antibodies against gelsolin (No. 2, BD Bioscience, San Jose, CA), osteonectin (AON-1, Developmental Studies Hybridoma Bank), collagen XV[25] (DB-157.F1, provided by Dr. Pihlajaniemi, University of Oulu), fast-type myosin heavy chain (WB-MHCf, Novocastra, Newcastle upon Tyne, UK), and rabbit polyclonal antibody against collagen III (LSL Cosmobio, Tokyo, Japan).

Results. We performed cDNA microarray analyses on skeletal muscle RNA from eight genetically diagnosed XLMTM patients. The mutation data and muscle histology of these patients in this study are represented in table 1 and figure 1A. Myofibers in all XLMTM patients are very small, consist predominantly of type 1 fibers, and show accumulations of mitochondria in the center of the fibers. Fiber-sizes and fiber-type proportion varied among the patients. But in Patients 3 and 5, some fibers are relatively large and appear similar to control; however, some ATPase-positive fibers at pH 9.4 which are probably type 2 fibers were extremely small, presumably due to the disease status. For comprehensive gene expression analysis, we used our custom cDNA microarray and performed competitive hybridization with two targets, which were prepared from an RNA extracted from biopsied muscle and a commercially available control RNA. Spots giving low signals for both targets on each array were excluded from further analyses by the filtration method. Of the 5,670 probes, 1,533 in each array failed to hybridize and were excluded. By hierarchical clustering analysis for the filtrated 4,227 probes with Pearson correlation by Gene Spring software, expression levels of muscle genes in XLMTM patients were clearly distinct from controls (figure 1B).

To characterize gene expression in XLMTM muscles, we compared collective average expression data to those of other muscular disorders and controls by hierarchical clustering analysis. We classified gene expression in XLMTM into branches distinct from congenital muscular dystrophies, progressive muscular dystrophies, and controls (figure 1C). These expression data clearly represent the unique pathologic characters of XLMTM muscles at the molecular level. To deduce the pathognomonic features of gene expression, we performed statistical group comparison between collective data from all XLMTM patients and controls. We identified 199 probes representing 183 genes with significant change by parametric Welch t test with $p < 0.0001$. Among the 183 genes, 120 genes were upregulated with increased expression, while 63 genes were downregulated with decreased expression as shown in table E-1 (available on the *Neurology* Web site at www.neurology.org). To characterize the gene expression in XLMTM muscles, we further categorized these genes by cellular function (see table E-1). The upregulated group was predominantly comprised of genes encoding cytoskeletal proteins and extracellular matrix (ECM)/sarcolemmal proteins. In contrast, genes involved with energy metabolism and muscle contraction were principally downregulated. Almost all of the genes encoding glycolytic pathway enzymes and several genes in TCA cycle were downregulated, whereas the genes encoding the enzymes in respiratory chain in mitochondria were unchanged. We also observed that genes expressed in type 1 fibers have the tendency to be upregulated, while those in type 2 fibers were downregulated, reflecting the pathologic features of XLMTM. Interestingly, genes related to muscle atrophy such as atrogin-1 (*FBXO32*) and forkhead box transcriptional factor gene (*FOXO1A*),[26-29] or those of proteolytic pathways, were not upregulated. Only a few genes related to membrane trafficking showed changes in their expression.

Since the skeletal muscle fibers with XLMTM show characteristic structural features such as small rounded shape, centrally located nuclei, and mitochondrial accumu-

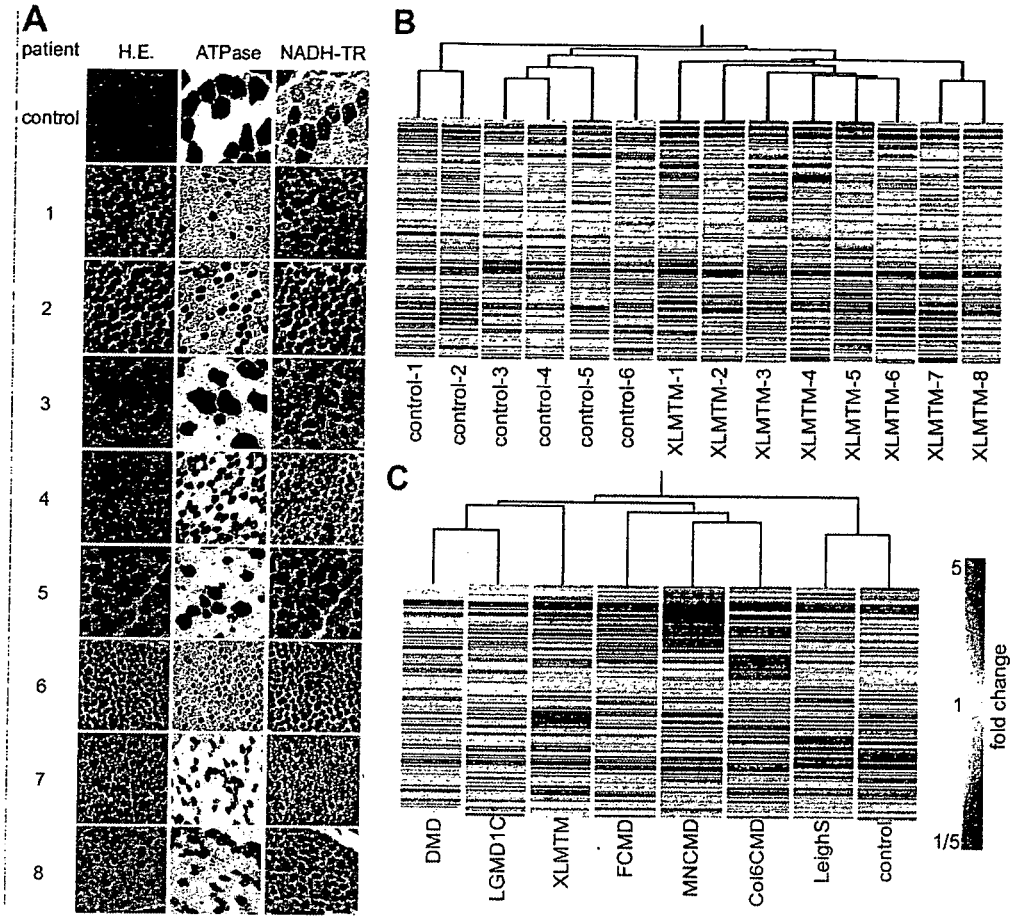

Figure 1. Muscle pathology of XLMTM patients and hierarchical analyses of gene expression among the patients and muscular disorders. (A) Muscles were stained with hematoxylin-eosin (HE), myosin-ATPase in pH 9.4 (ATPase) and NADH-tetrazolium reductase (NADH-TR). Bar denotes 10 μm. (B) Hierarchical analysis of gene expression among XLMTM patients and control individuals using pre- filtrated 4,227 probe data. (C) Hierarchical analysis of gene expression among hereditary muscle disorders. Each genetically or immunohistochemically diagnosed specimen with various disorders was analyzed with same cDNA arrays. The expression data were separately assembled in each disorder and statistically analyzed. The disorders used for comparison are as follows: DMD = Duchenne muscular dystrophy; LGMD1C = limb-girdle muscular dystrophy type 1C; FCMD = Fukuyama-type congenital muscular dystrophy; MNCMD = merosin-negative congenital muscular dystrophy; Col6CMD = collagen VI-deficient congenital muscular dystrophy; LeighS = Leigh syndrome; control = age-matched diseased control.

lations in the center, we hypothesized that these structural alterations of myofibers may be caused by the reconstruction of intracellular and extracellular molecular architectures. Therefore, we focused on the expression of genes encoding cytoskeletal proteins and ECM/sarcolemmal proteins. Table 2 shows the expression data of genes with significant changes in these categories. The ECM/sarcolemmal protein genes showed more dynamic expression changes than cytoskeletal protein genes. Among cytoskeletal protein genes showing increased expression several are related to remodeling of actin network, such as *MARCKS, CFL1, GSN, PFN1, PFN2, TAGLN, ACTR3,* and *PHACTR4*. These gene products play roles in crosslinking, severing, capping, and depolymerization of actin filaments, as well as stabilization of globular actin molecules.[50] In contrast, the downregulated genes, *DCTN2, MAPT,* and *TTL*, encode microtubule interacting proteins. We confirmed the microarray finding of increased *GSN* gene expression at the mRNA level by quantitative RT-PCR and at protein level by Western blotting, and also examined the distribution of its protein product, gelsolin, in skeletal muscles with XLMTM. The gelsolin transcript was upregulated 4.5-fold and the protein was increased 4-fold in XLMTM muscles as compared with control (figure 2A). Immunohistochemical data showed prominent staining in extremely small areas (arrows in figure 2, B and C). We found that these small areas are atrophic type 2 fibers by immunostaining using anti-fast-type myosin heavy chain antibody. Gelsolin was also detected in the central region, around nuclei of atrophic small fibers, although it was undetectable in control muscles (arrows in figure 2D). Among the ECM and sarcolemmal protein genes, collagen genes (*COL3A1* and *COL15*) and osteoblast-related genes (*ON* and *OSF2A*) showed strong upregulation, whereas muscle-specific membrane protein genes (*SNTA1, SGCA,* and *DYSF*) were downregulated. We also confirmed the upregulation of osteonectin, the *ON* gene product, in mRNA (7.6-fold) and protein (2.4 fold) (figure 2E). Immu-

Table 2 Expression change of cytoskeleton- and ECM/sarcolemmal-related genes in X-linked myotubular myopathy (XLMTM)

Cytoskeleton-related genes			ECM/sarcolemmal-related genes		
Gene	Accession	Fold change	Gene	Accession	Fold change
CFL1	NM_005507	3.93	COL3A1	NM_000090	12.51
PFN2	NM_002628	3.44	ON	NM_003118	8.39
K-ALPHA-1	NM_006082	3.28	OSF-2	NM_006475	4.67
DMD	NM_000109	3.23	DAG1	NM_004393	3.68
MACS	NM_002356	3.20	MGC3047	NM_032348	3.48
TAGLN	NM_003186	3.08	COL15A1	NM_001855	3.36
PFN1	NM_005022	2.92	LUM	NM_002345	3.18
MYH9	NM_002473	2.49	GPC1	NM_002081	2.15
VIM	NM_003380	2.42	SPARCL1	NM_004684	2.11
LMO7	NM_015843	2.30	SLMAP	NM_007159	2.05
GSN	NM_000177	2.26	SPON2	NM_012445	1.31
ACTR3	NM_005721	2.02			
PHACTR4	NM_023923	1.96			
DOC1	NM_014890	0.66	DYSF	NM_003494	0.58
TPM3	NM_152263	0.55	SGCA	NM_000023	0.36
NRAP	NM_006175	0.49	SNTA1	NM_003098	0.29
MYH14	NM_024729	0.49			
MAPT	NM_016835	0.46			
TTL	NM_153712	0.37			

The expression change is represented by ratio calculated by division of the average expression value of eight XLMTM patients with that of six age-matched control individuals.

nohistochemistry showed enhanced osteonectin staining around the atrophic fibers in XLMTM muscles (data not shown). Collagen XV and III were expressed in sarcolemma, endomysium, and strongly in capillaries (arrowheads in figure 2, F and I). In addition, both collagens showed increased expression around small atrophic fibers (arrows in figure 2, G, H, J, and K). We also confirmed the data of the other eight genes on microarray analysis by Western blotting as shown in figure E-1.

Discussion. In this study, we comprehensively analyzed gene expression in skeletal muscle from genetically confirmed XLMTM patients using cDNA microarray and identified the set of genes showing significant changes in expression specific to this disease. One of the most striking changes in gene expression in XLMTM is downregulation of the genes in energy metabolism, especially those involved in glycolytic pathway. Our previous expression analysis in Duchenne muscular dystrophy also showed the downregulation of genes in energy metabolism; however, a wider variety of genes including the genes in TCA cycle and respiratory chain were also mildly affected.[21] The marked downregulation of genes in glycolytic pathway also has been reported in nemaline myopathy, therefore, thus may be a common feature in congenital myopathies in general.

A *MTM1* gene-knockout mouse initially shows normal early development but later develops severe atrophy and disorganization of organelle distribution in myofibers.[10] Several previous studies have described gene expression mechanisms inducing muscle atrophy or wasting observed in various human conditions such as disuse atrophy, diabetes, and cachexia.[31] In catabolic states, PI3k/Akt pathway is downregulated, leading to the activation of FOXO1A and to transcription of *FBXO32, MURF1,* and other genes that promote wasting.[26-28] However, in our analysis, neither significant upregulation of *FOXO* and *FBXO32* genes or downregulation of ribosomal S6 kinase and other genes involved in translational pathway was observed in XLMTM. Our preliminary results showed that phosphorylation levels of Akt-1 and its downstream signaling molecules in XLMTM muscles were similar to those in controls (Fujita et al., unpublished data). These data strongly suggest that neither inactivation of PI3k/Akt pathway nor activation of FOXO/FBXO32 was involved in the muscle fiber atrophy in XLMTM.

We also found that several genes encoding cytoskeletal proteins were significantly upregulated, including those encoding actin-interacting proteins such as *GSN, MACS, LMO7, TAGLN, CFL1, PFN1, PFN2, ACTR3,* and *PHACTR4*. Increased expression of actin assembly and disassembly regulatory proteins has been observed in association with dynamic changes of cell shape such as morphogenesis and remodeling of cells and tissues in cell differentiation, development, and tumorigenesis.[30] Interestingly, a

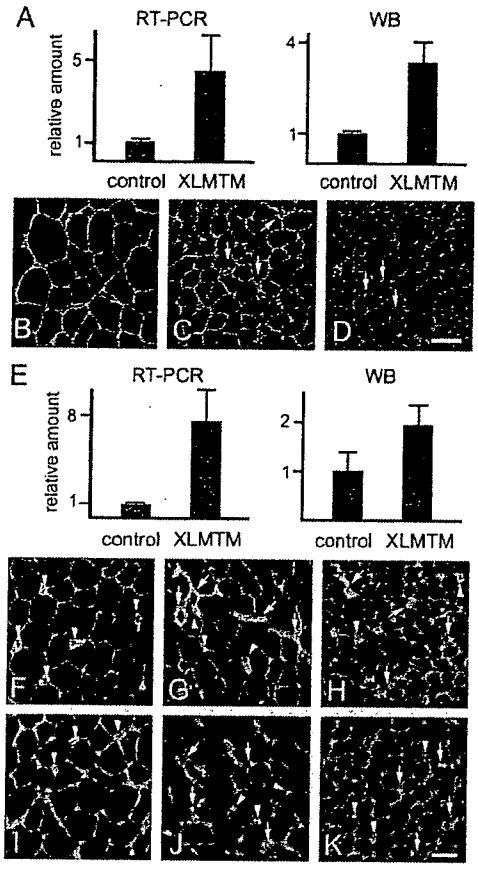

Figure 2. Expression analyses of gene products of gelsolin, osteonectin, COL15, and COL3 genes in XLMTM muscles. (A) Quantitative RT-PCR and Western blot (WB) analyses of gene products of gelsolin genes. Expression levels are represented as relative value to control. RT-PCR: control, n = 4; XLMTM, n = 7, Western blot: control, n = 4; XLMTM, n = 5. (B–D) Immunohistochemical staining of gelsolin in skeletal muscles with control (B) and XLMTM (C, Patient 5; D, Patient 7). Green, gelsolin, Red, sarcospan, counter staining of sarcolemma. Bar denotes 10 μm. (E) Quantitative RT-PCR and Western blot (WB) analyses of gene products of ON gene. Expression levels are represented as relative value to control. RT-PCR: control, n = 4; XLMTM, n = 7, Western blot: control, n = 4; XLMTM, n = 5. (F–K) Immunohistochemical staining of collagen XV (F–H) and collagen III (I–K) in skeletal muscles with control (F and I) and XLMTM (Patients 5, G and J; Patient 7, H and K). Bar denotes 10 μm.

previous report showed that myotubularin localizes to Rac1-inducible plasma membrane ruffles and to filopodia.[13] Rac1 activation induces membrane ruffling, via activation of WAVE2/SCAR2. WAVE2 is involved in the formation of branched actin filament meshwork in membrane ruffles by activating Arp2/3 complex, which consists of ACTR3 and other proteins.[32] Furthermore, strong expression of gelsolin was observed in extremely atrophic fibers and the center of small rounded myofibers in XLMTM. Our results showing upregulation of actin-filament remodeling protein genes raise the possibility that myotubularin may be a regulator of membranous cytoskeletal actin-network, moreover, with a deficiency of myotubularin, actin filament disassembly may be induced, resulting in remodeling of cell morphology and organelle distribution in myofibers.

Several genes encoding ECM/sarcolemma proteins are also upregulated in XLMTM muscles. The upregulation of osteoblast-related genes was remarkable. The expression of *ON* protein products, osteonectin and its related protein, osteopontin, were expressed around small atrophic fibers (Fujita et al., unpublished data). The osteopontin has been reported to be upregulated in the regenerating process in muscles and is expressed by macrophages. Although no apparent degeneration-regeneration of myofibers has been observed in XLMTM, the expression of these molecules suggests the presence of certain infiltrating cells in endomysium around atrophic fibers. *COL3* and *COL15* were significantly upregulated and the protein products of these genes strongly expressed in sarcolemma and endomysium, especially around small fibers. These results suggest that the morphologic changes of myofibers in XLMTM stimulate connective tissue growth in endomysium around atrophic fibers.

By comprehensive gene expression analysis of XLMTM, we have identified specific molecular features in XLMTM. The gene expression may partly explain the unique clinical and pathologic features in XLMTM. The transcriptional alterations in XLMTM indicate downregulation of the muscle contraction and energy production systems with increased dynamic reconstruction of intracellular and extracellular framework of myofibers. Our microarray collection of more than 4,200 genes is based on database information about skeletal muscle expression. These genes are not only skeletal muscle-specific genes but also encode a variety of proteins or genes predominantly expressed in the other organs; nevertheless, they do not cover all of the human transcripts. Total transcriptome expression analysis may supply more information to account for the pathomechanism of XLMTM.

Acknowledgment

The authors thank Drs. Y.K. Hayashi and I. Nonaka (National Center of Neurology and Psychiatry) for their critical comments and discussion on the manuscript, and Drs. M. Hirano (Columbia University) and M.C. Malicdan (National Center of Neurology and Psychiatry) for reviewing the manuscript. The monoclonal antibody AON-1, developed by Dr J.D. Termine, was obtained from the Developmental Studies Hybridoma Bank developed under the auspices of the NICHD, NIH, and maintained by The University of Iowa, Department of Biologic Science, Iowa City.

References

1. Fardeau M, Tome FMS. Congenital myopathies. In: Engel AG, Franzini-Armstrong C, eds. Myology, 2nd ed. New York: McGraw-Hill, 1994;1487–1532.
2. Wallgren-Pettersson C, Clarke A, Samson F, et al. The myotubular myopathies: differential diagnosis of the X linked recessive, autosomal dominant, and autosomal recessive forms and present state of DNA studies. J Med Genet 1995;32:673–679.
3. Laporte J, Hu LJ, Kretz C, et al. A gene mutated in X-linked myotubu-

lar myopathy defines a new putative tyrosine phosphatase family conserved in yeast. Nat Genet 1996;13:175–182.
4. Laporte J, Biancalana V, Tanner SM, et al. MTM1 mutations in X-linked myotubular myopathy. Hum Mutat 2000;15:393–409.
5. Herman GE, Kopacz K, Zhao W, Mills PL, Metzenberg A, Das S. Characterization of mutations in fifty North American patients with X-linked myotubular myopathy. Hum Mutat 2002;19:114–121.
6. Biancalana V, Caron O, Gallati S, et al. Characterisation of mutations in 77 patients with X-linked myotubular myopathy, including a family with a very mild phenotype. Hum Genet 2003;112:135–142.
7. Nishino I, Minami N, Kobayashi O, et al. MTM1 gene mutations in Japanese patients with the severe infantile form of myotubular myopathy. Neuromuscul Disord 1998;8:453–458.
8. Mandel JL, Laporte J, Buj-Bello A, Sewry C, Wallgren-Pettersson C. In: Karpati G, ed. Structural and molecular basis of skeletal muscle diseases. Basel: ISN Neuropath Press, 2002;124–129.
9. Spiro AJ, Shy GM, Gonatas NK. Myotubular myopathy. Persistence of fetal muscle in an adolescent boy. Arch Neurol 1966;14:1–14.
10. Buj-Bello A, Laugel V, Messaddeq N, et al. The lipid phosphatase myotubularin is essential for skeletal muscle maintenance but not for myogenesis in mice. Proc Natl Acad Sci USA 2002;99:15060–15065.
11. Blondeau F, Laporte J, Bodin S, Superti-Furga G, Payrastre B, Mandel JL. Myotubularin, a phosphatase deficient in myotubular myopathy, acts on phosphatidylinositol 3-kinase and phosphatidylinositol 3-phosphate pathway. Hum Mol Genet 2000;9:2223–2229.
12. Schaletzky J, Dove SK, Short B, Lorenzo O, Clague MJ, Barr FA. Phosphatidylinositol-5-phosphate activation and conserved substrate specificity of the myotubularin phosphatilinositol 3-phosphatases. Curr Biol 2003;13:504–509.
13. Laporte J, Blondeau F, Gansmuller A, Lutz Y, Vonesch JL, Mandel JL. The PtdIns3P phosphatase myotubularin is a cytoplasmic protein that also localizes to Rac1-inducible plasma membrane ruffles. J Cell Sci 2002;115:3105–3317.
14. Nandurkar HH, Layton M, Laporte J, et al. Identification of myotubularin as the lipid phosphatase catalytic subunit associated with the 3-phosphatase adapter protein, 3-PAP. Proc Natl Acad Sci USA 2003; 100:8660–8665.
15. Leevers SJ, Vanhaesebroeck B, Waterfield MD. Signaling through phosphoinositide 3-kinases: the lipids take centre stage. Curr Opin Cell Biol 1999;11:219–225.
16. Rameh LE, Cantley LC. The role of phospahoinositide 3-kinase lipid products in cell function. J Biol Chem 1999;274:8347–8350.
17. Tsujita K, Itoh T, Ijuin T, et al. Myotubularin regulates the function of the late endosome through the gram domain-phosphatidylinositol 3,5-bisphosphate interaction. J Biol Chem 2004;279:13817–13824.
18. Chen YW, Zhao P, Borup R, Hoffman EP. Expression profiling in the muscular dystrophies: identification of novel aspects of molecular pathology. J Cell Biol 2000;151:1321–1336.
19. Bakay M, Zhao P, Chen J, Hoffman EP. A web accessible complete transcriptome of normal human and DMD muscle. Neuromuscul Disord 2002;12:S125–S141.
20. Campanaro S, Romualdi C, Fanin M, et al. Gene expression profiling in dystrophinopathies using dedicated muscle microarray. Hum Mol Genet 2002;11:3283–3289.
21. Noguchi S, Tsukahara T, Fujita M, et al. cDNA microarray analysis of individual Duchenne muscular dystrophy patients. Hum Mol Genet 2003;12:595–600.
22. Sanoudou D, Haslett JN, Kho AT, et al. Expression profiling reveals altered satellite cell numbers and glycolytic enzyme transcription in nemaline myopathy muscle. Proc Natl Acad Sci USA 2003;100:4666–4671.
23. Tsai T-C, Horinouchi H, Noguchi S, et al. Characterization of *MTM1* mutations in 31 Japanese families with myotubular myopathy, including a patient carrying 240 kb deletion in Xq28 without male hypogenitalism. Neuromuscul Disord 2005;15:245–252.
24. Hayashi YK, Ogawa M, Tagawa K, et al. Selective deficiency of α-dystroglycan in Fukuyama-type congenital muscular dystrophy. Neurology 2001;57:115–121.
25. Hagg PM Hagg PO, Peltonen S, Autio-Harmainen H, Pihlajaniemi T. Location of type XV collagen in human tissues and its accumulation in the interstitial matrix of the fibrotic kidney. Am J Pathol 1997;150: 2075–2086.
26. Sandri M, Sandri C, Gilbert A, et al. Foxo transcriptional factors induce the atrophy-related ubiquitin ligase atrogin-1 and cause skeletal muscle atrophy. Cell 2004;117:399–412.
27. Stitt TN, Drujan D, Clarke BA, et al. The IGF-1/PI3K/Akt pathway prevents expression of muscle atrophy-induced ubiquitin ligases by inhibiting FOXO transcription factors. Mol Cell 2004;14:395–403.
28. Cai D, Frantz JD, Tawa Jr, NE, et al. IKKβ/NF-κB activation causes severe muscle wasting in mice. Cell 2004;119:285–298.
29. Kamei Y, Miura S, Suzuki M, et al. Skeletal muscle FOXO1 (FKHR) transgenic mice have less skeletal muscle mass, down-regulated type I (slow twitch/red muscle) fiber genes, and impaired glycemic control. J Biol Chem 2004;279:41114–41123.
30. Kreis T, Vale R, eds. Guidebook to the cytoskeletal and motor proteins, 2nd ed. New York: Oxford University Press, 1999.
31. Glass DJ. Signalling pathways that mediate skeletal muscle hypertrophy and atrophy. Nat Cell Biol 2003;5:87–90.
32. Takenawa T, Miki H. WASP and WAVE family proteins: key molecules for rapid rearrangement of cortical actin filaments and cell movement. J Cell Sci 2001;114:1801–1809.

A new congenital form of X-linked autophagic vacuolar myopathy

Abstract—In a new family with X-linked congenital autophagic vacuolar myopathy (AVM), seven affected boys presented with congenital hypotonia, dyspnea, and dysphagia with delayed motor milestones. Muscle pathology revealed autophagic vacuoles with sarcolemmal features, multilayered basal lamina with marked sarcolemmal deposition of C5-9 membrane attack complex and calcium, histologically indistinguishable from childhood-onset X-linked myopathy with excessive autophagy (XMEA). Haplotype analysis suggests that this new AVM and XMEA may be allelic despite different clinical presentations.

NEUROLOGY 2005;65:1132–1134

C. Yan, MD; M. Tanaka, PhD; K. Sugie, MD, PhD; T. Nobutoki, MD; M. Woo, MD; N. Murase, MD, PhD; Y. Higuchi, MD, PhD; S. Noguchi, PhD; I. Nonaka, MD, PhD; Y.K. Hayashi, MD, PhD; and I. Nishino, MD, PhD

Autophagic vacuolar myopathy (AVM) is pathologically characterized by presence of autophagic vacuoles with sarcolemmal features (AVSF)—autophagic vacuoles with expression of virtually all sarcolemmal proteins and acetylcholinesterase (AChE).[1] Four forms of AVM with AVSF have been identified: Danon disease,[2] X-linked myopathy with excessive autophagy (XMEA),[3] infantile AVM,[4] and adult-onset AVM with multiorgan involvement.[5] Danon disease is an X-linked dominant disorder with LAMP-2 gene (LAMP-2) mutation on chromosome Xq24 resulting in a triad of skeletal myopathy, hypertrophic cardiomyopathy, and mild mental retardation.[2] XMEA, also known as X-linked vacuolated myopathy,[6] is slowly progressive, with no other organ involvement. Linkage analysis identified the XMEA locus in the most telomeric region of chromosome X.[7] Infantile AVM patients were floppy at birth, with myopathy and cardiomyopathy causing early death.[4] Recently, a patient with adult-onset AVM with multiorgan involvement (eyes, heart, liver, lung, kidney, and skeletal muscles) was reported. In this study, we describe a new Chinese-American family with a severe form of myopathy with AVSF.

From the Department of Neuromuscular Research (Drs. Yan, Tanaka, Sugie, Noguchi, Nonaka, Hayashi, and Nishino), National Institute of Neuroscience, National Hospital for Mental, Nervous and Muscular Disorders (Drs. Nobutoki and Nonaka), National Center of Neurology and Psychiatry, Kodaira, Tokyo; Dr. Woo's Pediatric Clinic (Dr. Woo), Kyoto; Departments of Neurology (Dr. Murase) and Pediatrics (Dr. Higuchi), National Hospital Organization Utano National Hospital, Kyoto, Japan; and Department of Neurology (Dr. Yan), Qilu Hospital of Shandong University, Jinan, China.

Supported partly by the Research on Health Sciences focusing on Drug Innovation and the Research on Psychiatric and Neurologic Diseases and Mental Health from the Japanese Health Sciences Foundation; partly by a Grant-in-Aid for Scientific Research from the Japan Society for the Promotion of Science; and partly by a Research Grant (17A-10) for Nervous and Mental Disorders from the Ministry of Health, Labor and Welfare.

Disclosure: The authors report no conflicts of interest.

Received February 17, 2005. Accepted in final form June 20, 2005.

Address correspondence and reprint requests to Dr. Ichizo Nishino, Department of Neuromuscular Research, National Institute of Neuroscience, National Center of Neurology and Psychiatry, 4-1-1 Ogawa-Higashi, Kodaira, Tokyo 187-8502, Japan; e-mail: nishino@ncnp.go.jp

Methods. All clinical materials used were obtained with informed consent. Genomic DNA was isolated from peripheral lymphocytes using a standard technique. Muscle specimens were flash-frozen in isopentane chilled with liquid nitrogen for histologic analysis or fixed in 2% glutaraldehyde and postfixed in osmium tetroxide for electron microscopic analysis.

Seven male patients in this family presented with similar clinical symptoms (figure 1). Patient IV-2 (figure 1, C and D), a 7-year-old boy from nonconsanguineous Chinese-American parents, had congenital hypotonia and hypoventilation requiring respiratory support for 3 days. Because of difficulty suckling and dysphagia, nasogastric tube feeding was initiated until age 2½ years. The patient's motor milestones were delayed, with sitting at 9 months and walking with support at 2 years. Thereafter, his motor development deteriorated, with progressive muscle weakness and crawling at age 7 years. His serum creatine kinase (CK) level was increased at 1,962 IU/L (reference range = 51 to 197). Generalized muscle atrophy and weakness, including facial and neck muscles, were observed. He had a high-arched palate with normal mentation. EKG revealed incomplete right bundle-branch block, and echocardiography showed left ventricular hypertrophy. Needle EMG of the right biceps brachii revealed complex repetitive discharges without fibrillation potentials or positive sharp waves and low-amplitude, short-duration motor unit potentials with early recruitment, which are compatible with a chronic myopathic condition.

Patient IV-1 (figure 1, B and D) was the 9-year-old elder brother of the proband. He was also hypotonic at birth, with an increased CK level (2,000 IU/L). He also required nasogastric tube feeding until age 2 years. He sat at 8 months and walked at 21 months but became wheelchair bound at age 5 years. He had generalized muscle weakness and atrophy, including facial and neck muscles, with no cardiac or CNS involvement.

Two maternal uncles (III-2 and -3) had asphyxia and died immediately after birth. Another maternal uncle (III-5) had a weak cry and died at age 8 months. Two maternal grandmother's brothers (II-3 and -4) died within several months after birth because of difficulty suckling. No female relatives had clinical signs of myopathy, including the mother (III-4) of the index patients, with a normal CK level (39 IU/L).

Haplotyping and linkage analysis. Haplotype analysis of the genomic DNA from two affected (IV-1 and IV-2) and six unaffected family members (I-2, II-1, II-2, III-1, III-4 and III-6) (see figure 1) was performed using an ABI PRISM 310 genetic analyzer (PE Applied Biosystems, CA) with the following 23 microsatellite markers on chromosome X: Xpter-DXS1060-DXS8051-DXS987-DXS1226-DXS121-DXS1068-DXS993-DXS991-DXS986-DXS990-DXS458-DXS1106-DXS8096-DXS8055-DXS1001-DXS1047-DXS691-DXS1227-DXS8043-DXS1215-DXS8091-DXS8069-DXS1073-Xqter. The multipoint linkage analysis from the haplotype data were conducted using GENEHUNTER.[8]

Sequence analysis. Mutation analysis of LAMP-2 was performed in two affected patients (IV-1 and IV-2) using an ABI PRISM 3100 automated sequencer (PE Applied Biosystems), as described.[2]

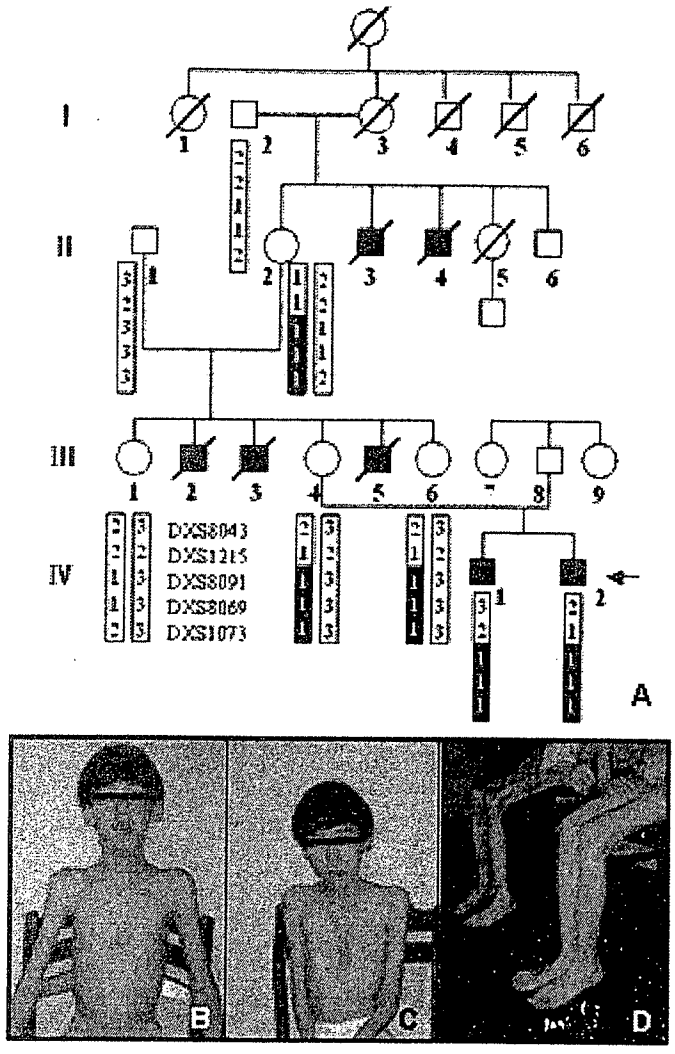

Figure 1. In the pedigree of the family (A), shaded boxes are the affected members. Symbols with diagonal lines represent deceased individuals. In the haplotype chart of this family, only informative regions (Xq27.2 to Xqter) are presented. The most important candidate region containing a common haplotype in three generations is highlighted by shaded boxes. Patient IV-2 (B and D) and Patient IV-1 (C and D) showed facial and neck muscle involvement, thoracic cage deformity, and severe generalized muscle atrophy.

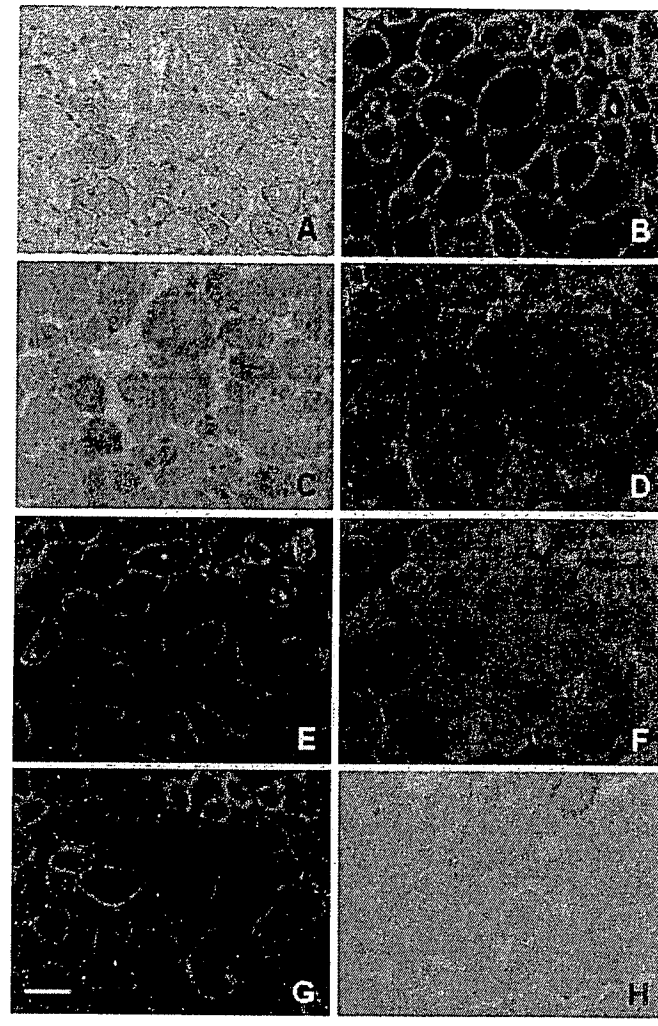

Figure 2. Muscle pathologic features (Patient IV-2). The vacuolar membranes have increased acetylcholinesterase (AChE) activities (A), and dystrophin is expressed in most intrasarcoplasmic vacuolar membranes (B). Strong acid phosphatase activity is observed inside vacuoles (C). Increased immunoreactivity of LAMP-2 is seen both at the surface membranes and within the cytoplasm of affected fibers (D). LIMP-1/CD63 is strongly stained at the sarcolemma and within the cytoplasm (E), and some cytoplasmic granular staining is colocalized with LC3 (F). Marked C5-9 membrane attack complex deposition is seen at the sarcolemma of almost all muscle fibers (G). By alizarin red, calcium deposition is seen at the sarcolemma and occasionally within the cytoplasm (H). Bar = 30 μm.

Histochemical and immunohistochemical analyses and electron microscopic studies. Serial frozen sections were stained with a battery of histochemical methods including hematoxylin and eosin (H-E), modified Gomori-trichrome, acid phosphatase, AChE, nonspecific esterase (NSE), periodic acid–Schiff, and alizarin red.

Immunohistochemical analysis was done using antibodies for LAMP-2 (H4B4; Developmental Studies Hybridoma Bank [DSHB]), LIMP-1/CD63 (H5C6; DSHB), dystrophin (NCL-DYS1; Novocastra Laboratories), C5b-9 membrane attack complex (MAC; DAKO Co.), microtubule-associated protein 1 light chain (LC3; kindly provided by Dr. Ueno[9]), CD59 (Biogenesis, Ltd.), dystrophin (NCL-DYS2; Novocastra), dysferlin (NCL-Hamlet 2; Novocastra), alpha sarcoglycan (Novocastra), caveolin-3 (Transduction Laboratories), and merosin (Chemicon International).

Electron microscopy was performed using a Hitachi H-7100 electron microscope.

Results. The skeletal muscle from patient IV-2 showed marked variation in fiber size with endomysial fibrosis. There are many intracytoplasmic vacuoles with activity for NSE (data not shown) and AChE (figure 2, A). Positive immunoreaction was observed at the vacuolar membranes with all five antibodies for sarcolemmal and extracellular matrix protein including dystrophin (figure 2, B). Within vacuoles, strong acid phosphatase activity was seen (figure 2, C), and vacuolar membranes showed LAMP-2 staining (figure 2, D), indicating the lysosomal nature of the vacuoles. Strong immunoreaction to LIMP-1/CD63, a lysosomal membrane protein, was observed both at the sarcolemma and inside the vacuoles (figure 2, E). LC3, having a crucial role for autophagosome formation,[9] was abundant in the cytoplasm, and some colocalized with LIMP-1/CD63 (figure

Figure 3. Electron microscopy shows large accumulation of dense globes and amorphous granules surrounded by a single layer membrane under sarcolemma or between the multiple layered basal lamina (white arrows). Some of these dense globes are encircled by a double-layered membrane (arrows). Some vacuoles are attached to the sarcolemma indicating exocytotic process. Bar = 1 μm.

2, F). MAC (figure 2, G) and calcium (figure 2, H) were markedly deposited at the sarcolemma in most fibers. CD59, an inhibitor of MAC, was positive in all muscle fibers, including MAC-positive ones (data not shown). Muscles from patients with Danon disease did not stain for LAMP-2. Membrane staining of LIMP-1/CD63 was weak, and MAC deposition was rarely observed (data not shown).

Electron microscopy of the patients' muscles revealed that numerous electron dense granules accumulated in various sizes of intracytoplasmic vacuoles (figure 3). Some larger granules were surrounded by double-layered membrane. The severely affected muscle fibers were surrounded by multilayered basal lamina wherein dense granules were also observed.

Mapping of the disease in this family using polymorphic microsatellite markers spanning the entire X-chromosome showed the highest multipoint lod score peak of 0.46 between markers DXS8069 and DXS1073. Other X chromosome region showed negative lod score, except for the small regions around DXS1226 (maximum 0.14) and DXS458 (maximum 0.08), suggesting that the causative gene may be localized in Xq28 (distal to DXS1215) (figure 1, A).

No mutation in *LAMP-2* was identified in the two affected patients examined.

Discussion. XMEA is clinically characterized as slowly progressive or nonprogressive myopathy with AVSF. The onset of symptoms usually ranges between ages 5 and 10 years, presenting with difficulty in climbing stairs and running without loss of ambulation. Lifespan is not altered. In contrast, our patients have more severe clinical manifestations with infantile hypotonia, dyspnea, and dysphagia. Some of the relatives died in early infancy, probably because of the same disease. Nevertheless, the pathologic features of our patients—multilayered basal lamina and intense sarcolemmal deposition of MAC and calcium in addition to AVSF—have been described as pathognomonic of XMEA.[6,10] In fact, the disease is pathologically indistinguishable from XMEA, suggesting allelism to XMEA. This notion is supported by the facts that the disease is transmitted through an X-linked recessive inheritance pattern and that haplotype analysis suggested Xq28, the chromosomal region for XMEA,[7] as a possible locus of this disease. The low lod score is due to small family size. Furthermore, similar pathologic findings were also reported in infantile AVM,[4] suggesting that it may also be allelic to XMEA. The identification of the XMEA gene will resolve the issue of allelism of these disorders to XMEA.

Although the genetic cause is still unknown, colocalization of LC3 and LIMP-1/CD63 in the patients' muscles, together with numerous dense granules on electron microscopy, suggests abnormal protein degradation as part of the pathomechanism in infantile AVSF as well as in XMEA.

Acknowledgment

The authors thank the patients and their families for their cooperation, Dr. Takashi Ueno (Jutendo University, Tokyo, Japan) for providing the LC3 antibody, Dr. Michio Hirano (Columbia University, New York, NY) for reviewing the manuscript, Dr. Jun Kimura (University of Iowa, Iowa City, IA) for comments on EMG findings, and Dr. Mina Astejada (National Center of Neurology and Psychiatry, Kodaira, Tokyo, Japan) for comments on the manuscript.

References

1. Sugie K, Noguchi S, Kozuka Y, et al. Autophagic vacuoles with sarcolemmal features delineate Danon disease and related myopathies. J Neuropathol Exp Neurol 2005;64:513–522.
2. Nishino I, Fu J, Tanji K, et al. Primary LAMP-2 deficiency causes X-linked vacuolar cardiomyopathy and myopathy (Danon disease). Nature 2000;406:906–910.
3. Saviranta P, Lindlof M, Lehesjoki AE, et al. Linkage studies in a new X-linked myopathy, suggesting exclusion of DMD locus and tentative assignment to distal Xq. Am J Hum Genet 1988;42:84–88.
4. Yamamoto A, Morisawa Y, Verloes A, et al. Infantile autophagic vacuolar myopathy is distinct from Danon disease. Neurology 2001;57:903–905.
5. Kaneda D, Sugie K, Yamamoto A, et al. A novel form of autophagic vacuolar myopathy with late-onset and multi-organ involvement. Neurology 2003;61:128–131.
6. Villanova M, Louboutin JP, Chateau D, et al. X-linked vacuolated myopathy: complement membrane attack complex on surface membrane injured muscle fibers. Ann Neurol 1995;37:637–645.
7. Minassian BA, Aiyar R, Alic S, et al. Narrowing in on the causative defect of an intriguing X-linked myopathy with excessive autophagy. Neurology 2002;59:596–601.
8. Kruglyak L, Daly MJ, Reeve-Daly MP, Lander ES. Parametric and nonparametric linkage analysis: a unified multipoint approach. Am J Hum Genet 1996;58:1347–1363.
9. Anasuma K, Tanida I, Shirato I, et al. MAP-LC3, a promising autophagosomal marker, is processed during the differentiation and recovery of podocytes from PAN nephrosis. FASEB J 2003;17:1165–1167.
10. Louboutin JP, Villanova M, Lucas-Heron B, Fardeau M. X-linked vacuolated myopathy: membrane attack complex deposition on muscle fiber membranes with calcium accumulation on sarcolemma. Ann Neurol 1997;41:117–120.

PERGAMON

Neuromuscular Disorders 15 (2005) 336–341

www.elsevier.com/locate/nmd

Proteolysis of β-dystroglycan in muscular diseases

Kiichiro Matsumura[a,*], Di Zhong[a], Fumiaki Saito[a], Ken Arai[a], Katsuhito Adachi[b], Hisaomi Kawai[c], Itsuro Higuchi[d], Ichizo Nishino[e], Teruo Shimizu[a]

[a]*Department of Neurology and Neuroscience, Teikyo University School of Medicine,2-11-1 Kaga Itabashi-ku, Tokyo 173-8605, Japan*
[b]*Department of Internal Medicine, Tokushima National Hospital, 1354 Shikiji, Kamojima-cho, Oe-gun, Tokushima 776-8585, Japan*
[c]*Takamatsu Municipal Hospital,2-36-1 Miyawaki-cho, Takamatsu, Kagawa 760-8538, Japan*
[d]*Third Department of Internal, Medicine, Kagoshima University of Graduate School of Medical and Dental Sciences, 8-35-1 Sakuragaoka, Kagoshima, Kagoshima 890-8544, Japan*
[e]*Department of Neuromuscular, Research, National Institute of Neuroscience, 4-1-1 Ogawahigashi-cho, Kodaira, Tokyo187-8502, Japan*

Received 22 November 2004; received in revised form 5 January 2005; accepted 11 January 2005

Abstract

α-Dystroglycan is a cell surface peripheral membrane protein which binds to the extracellular matrix (ECM), while β-dystroglycan is a type I integral membrane protein which anchors α-dystroglycan to the cell membrane via the N-terminal extracellular domain. The complex composed of α-and β-dystroglycan is called the dystroglycan complex. We reported previously a matrix metalloproteinase (MMP) activity that disrupts the dystroglycan complex by cleaving the extracellular domain of β-dystroglycan. This MMP creates a characteristic 30 kDa fragment of β-dystroglycan that is detected by the monoclonal antibody 43DAG/8D5 directed against the C-terminus of β-dystroglycan. We also reported that the 30 kDa fragment of β-dystroglycan was increased in the skeletal and cardiac muscles of cardiomyopathic hamsters, the model animals of sarcoglycanopathy, and that this resulted in the disruption of the link between the ECM and cell membrane via the dystroglycan complex. In this study, we investigated the proteolysis of β-dystroglycan in the biopsied skeletal muscles of various human muscular diseases, including sarcoglycanopathy, Duchenne muscular dystrophy (DMD), Becker muscular dystrophy, Fukuyama congenital muscular dystrophy, Miyoshi myopathy, LGMD2A, facioscapulohumeral muscular dystrophy, myotonic dystrophy and dermatomyositis/polymyositis. We show that the 30 kDa fragment of β-dystroglycan is increased significantly in sarcoglycanopathy and DMD, but not in the other diseases. We propose that the proteolysis of β-dystroglycan may contribute to skeletal muscle degeneration by disrupting the link between the ECM and cell membrane in sarcoglycanopathy and DMD.

Keywords: Dystroglycan; Sarcoglyan; Dystrophin; Laminin; Extracellular matrix; Matrix metalloproteinase; Sarcoglycanopathy; Duchenne muscular dystrophy

1. Introduction

The dystroglycan complex is a cell membrane-spanning complex composed of α-and β-dystroglycan, which are encoded by a single gene *Dag1* and cleaved into two proteins by posttranslational processing [1]. α-Dystroglycan is a cell surface peripheral membrane protein which binds to laminin in the basement membrane, while β-dystroglycan is a type I integral membrane protein which anchors α-dystroglycan to the cell membrane via the N-terminus of the extracellular domain and binds to the cytoskeletal protein dystrophin via the C-terminal cytoplasmic domain [1–5]. Thus, the dystroglycan complex provides a tight link between the extracellular matrix (ECM) and intracellular cytoskeleton. Recently, we reported a matrix metalloproteinase (MMP) activity that disrupts the dystroglycan complex by cleaving the extracellular domain of β-dystroglycan specifically [6]. This MMP creates a characteristic 30 kDa fragment of β-dystroglycan (β-DG_{30}) that is detected by the monoclonal antibody 43DAG/8D5 directed against the C-terminus of β-dystroglycan [6].

In the previous study, we showed that β-DG_{30} was increased in the skeletal and cardiac muscles of cardiomyopathic hamsters [7], the model animals of sarcoglycanopathy (SGCP) [8,9], and that this resulted in the disruption of the link

* Corresponding author. Tel.: +81 3 3964 1211x1915; fax: +81 3 3964 6394.
E-mail address: k-matsu@med.teikyo-u.ac.jp (K. Matsumura).

0960-8966/$ - see front matter © 2005 Elsevier B.V. All rights reserved.
doi:10.1016/j.nmd.2005.01.007

between the ECM and cell membrane via the dystroglycan complex in these tissues [7]. In the present study, we investigated the proteolysis of β-dystroglycan in the biopsied skeletal muscles of various human muscular diseases. We show that β-DG_{30} is increased significantly in SGCP and Duchenne muscular dystrophy (DMD), but not in the other diseases.

2. Materials and methods

2.1. Patients

Tables 1 and 2 summarize the patients investigated in this study. The skeletal muscle specimens were obtained by diagnostic biopsy. The diseases include SGCP, DMD, Becker muscular dystrophy (BMD), Fukuyama congenital muscular dystrophy (FCMD), Miyoshi myopathy (MM), LGMD2A, facioscapulohumeral muscular dystrophy (FSHD), myotonic dystrophy (DM) and dermatomyositis/

Table 1
Summary of the patients and results of immunoblot analysis of β-dystroglycan in the skeletal muscle biopsy specimens

Diagnosis	No.	Age	Sex	β-DG_{30}/ β-DG_{full}	Average ± SE
Normal control	1	13	M	0.0358	0.0538 ± 0.0165
	2	14	M	0.0496	
	3	15	M	0.0411	
	4	15	M	0.0127	
	5	16	M	0.0823	
	6	40	M	0.0228	
	7	41	M	0.0253	
	8	43	F	0.0125	
	9	59	M	0.0687	
	10	62	M	0.1869	
SGCP	1	10M	F	2.1467	0.6801 ± 0.2299
	2	7	F	0.3227	
	3	8	M	0.2978	
	4	13	F	0.6819	
	5	15	F	1.0325	
	6	17	F	0.2721	
	7	18	F	0.2500	
	8	31	F	0.4374	
DMD	1	4M	M	0.3729	0.4540 ± 0.0944
	2	1	M	0.4553	
	3	1	M	0.4868	
	4	3	M	0.6436	
	5	3	M	0.3541	
	6	4	M	0.4800	
	7	4Y10M	M	0.3303	
	8	5	M	0.3762	
	9	5	M	0.5457	
	10	6	M	0.5272	
	11	7Y1M	M	0.5011	
	12	8Y9M	M	0.3745	
BMD	1	3	M	0.0309	0.1030 ± 0.0253
	2	3Y10M	M	0.1340	
	3	4Y7M	M	0.0585	
	4	5	M	0.1236	
	5	13	M	0.1681	
FCMD	1	7M	F	0.0218	0.0336 ± 0.0069
	2	8M	F	0.0213	
	3	9M	M	0.0599	
	4	9M	M	0.0421	
	5	9M	M	0.0204	
	6	1Y	F	0.0166	
	7	1Y5M	F	0.0658	
	8	3Y	F	0.0209	
MM	1	25	F	0.0991	0.0779 ± 0.0164
	2	27	M	0.0652	
	3	30	M	0.1313	
	4	38	M	0.0504	
	5	39	M	0.0436	
LGMD2A	1	7Y3M	F	0.0752	0.0646 ± 0.0148
	2	11	F	0.0794	
	3	20	M	0.0206	
	4	26	F	0.0832	
FSHD	1	8	M	0.1307	0.1048 ± 0.0234
	2	19	F	0.0966	
	3	25	M	0.1363	
	4	41	M	0.0170	
	5	48	M	0.1437	
DM	1	14	M	0.0652	0.0722 ± 0.0226
	2	28	M	0.0701	
	3	37	F	0.1541	
	4	50	F	0.0557	
	5	60	M	0.0161	
DM/PM	1	2Y5m	M	0.0762	0.0589 ± 0.0135
	2	3	F	0.0951	
	3	4	F	0.0602	
	4	4	M	0.0000	
	5	10	F	0.1340	
	6	23	M	0.0168	
	7	30	F	0.0114	
	8	33	F	0.0477	
	9	46	M	0.0512	
	10	51	F	0.0957	

The skeletal muscle biopsy specimens were analyzed by immunoblotting using the monoclonal antibody 43DAG/8D5 and the β-DG_{30}/β-DG_{full} ratio was obtained for each patient as described in Materials and Methods. SE, standard error.

Table 2
Genetic analysis of SGCP patients

Patient no	Genetic analysis
1	β-SG, 325 C to T (R109X), homozygous
2	β-SG, 325 C to T (R109X), homozygous
3	α-SG, 229 C to T (R77C), homozygous
4	γ-SG, 630-702 base deletion, homozygous
5	Not done
6	α-SG, 229 C to T (R77C), homozygous
7	α-SG, 220 C to T (R74W), homozygous
8	α-SG, 410 A to G (E137G)/409-423 bases insertion

Patient 5 was diagnosed as SGCP, based on the clinical profile and the specific deficiency of the components of the sarcoglycan complex in the biopsied skeletal muscle as revealed by immunohistochemical analysis (not shown).

polymyositis (DM/PM). The diagnoses were made based on the clinical features, histochemical and immunohistochemical analyses of skeletal muscle biopsy specimens. Genetic diagnoses were also made in some cases. The patients with no obvious pathological changes in the skeletal muscle specimens were included as normal controls.

2.2. Immunoblot analysis of β-dystroglycan in the biopsied skeletal muscles

The skeletal muscle specimens were extracted quickly by homogenizing and boiling in a buffer containing 80 mM Tris-HCl, pH 6.8, 10% SDS, 1% β-mercaptoethanol and 115 mM sucrose, in the presence of protease inhibitors, including 0.6 mg/ml pepstatin A, 0.5 mg/ml aprotinin, 0.5 mg/ml leupeptin, 1 mM benzamidine, 1 mM PMSF, 1 mM EDTA, 1 mM EGTA and 20 mg/ml N-Biphenylsulfonyl-phenylalanine hydroxamic acid (a kind gift from Shionogi & Co. Ltd), as described previously [6,7,10]. 3–15% SDS-polyacrylamide gel electrophoresis and immunoblotting were performed as described previously [6,7,10]. The proteolysis of β-dystroglycan was detected by the monoclonal antibody 43DAG/8D5 against the C-terminus of β-dystroglycan (a kind gift from Dr L. V. B. Anderson of Newcastle General Hospital) [6,7,11]. Immunoblot development was done by enhanced chemiluminescence (Pierce) and visualized by Image Station 440 system (Eastman Kodak Company, New Haven, CT). The band intensity of β-DG_{30} and the full-size 43 kDa β-dystroglycan (β-DG_{full}) was measured using 1D image analyzing software and the ratio of β-DG_{30} against β-DG_{full} (β-DG_{30}/β-DG_{full} ratio) was calculated for each patient. The average value of the β-DG_{30}/β-DG_{full} ratio was obtained for normal control and various muscular diseases. The statistical difference among the groups was first tested using one factor ANOVA and then the difference between normal control and each disease group was evaluated by Dunnett's analysis.

3. Results

The results are summarized in Table 1 and Fig. 1. The actual immunoblots of some of the patients are shown in Fig. 2. Although there was some variation among patients, a 30 kDa band corresponding to β-DG_{30} was clearly observed in all the patients with SGCP and DMD (Table 1 and Fig. 2). Statistical analysis demonstrated significant increase of the β-DG_{30}/β-DG_{full} ratio in SGCP and DMD, compared to normal control (Table 1 and Fig. 1). On the other hand, statistical analysis did not demonstrate significant increase of the β-DG_{30}/β-DG_{full} ratio in BMD, FCMD, MM, LGMD2A, FSHD, DM and DM/PM, compared to normal control (Table 1 and Fig. 1), although mild proteolysis was detectable in some individuals (Table 1 and Fig. 2).

We performed the histochemical analysis of skeletal muscle biopsy specimens in order to see if pathological changes were correlated with the increase of proteolysis of β-dystroglycan. The severity of the pathological changes

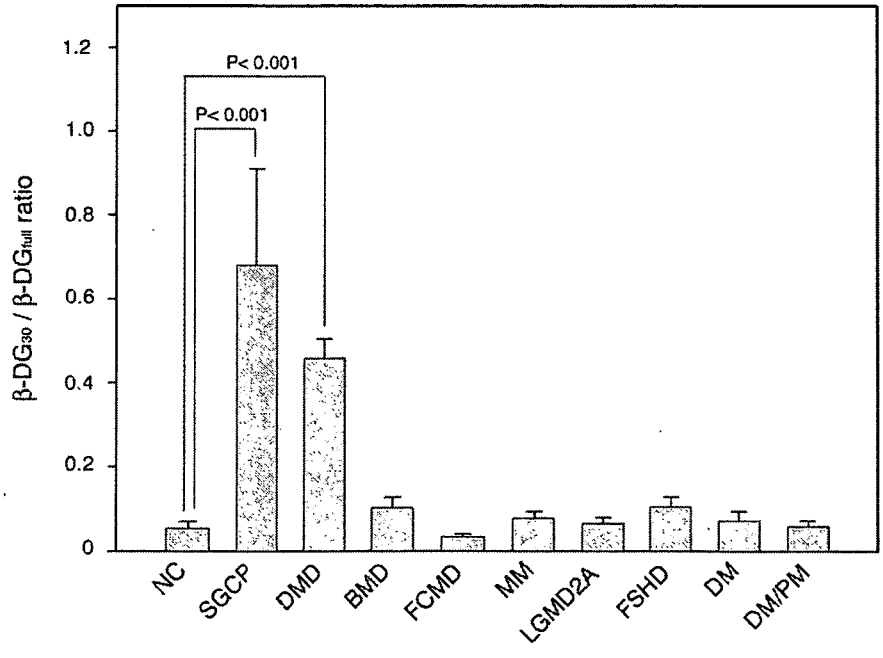

Fig. 1. The ratio of β-DG_{30} against β-DG_{full} in various muscular diseases.The average value of the β-DG_{30}/β-DG_{full} ratio was obtained for normal control and various muscular diseases. The statistical difference among the groups was first tested using one factor ANOVA and then the difference between normal control and each disease group was evaluated by Dunnett's analysis. The β-DG_{30}/β-DG_{full} ratio was significantly increased in SGCP ($P<0.001$) and DMD ($P<0.05$), compared to normal control. There was no significant difference between other disease groups and normal control. Error bar indicates standard error.